

(–)-Sandramycin: Total Synthesis and Characterization of DNA Binding Properties

Dale L. Boger,* Jyun-Hung Chen, and Kurt W. Saionz

Contribution from the Department of Chemistry, The Scripps Research Institute, 10666 North Torrey Pines Road, La Jolla, California 92037

Received August 14, 1995[⊗]

Abstract: Full details of the total synthesis of the potent antitumor antibiotic (–)-sandramycin (**1**), a cyclic decadepsipeptide possessing a 2-fold axis of symmetry, is described and constitutes the first total synthesis of a member of the growing class of naturally occurring agents now including the luzopeptins and quinaldopeptin. Key strategic elements of the approach include the late stage introduction of the heteroaromatic chromophore thereby providing access to analogs possessing altered intercalation capabilities, symmetrical pentadepsipeptide coupling and 32-membered macrocyclization conducted at the single secondary amide site in superb conversion (90%), and a convergent assemblage of the precursor pentadepsipeptide in which the potentially labile ester linkage was introduced in the final key coupling reaction. This approach also provided the cyclic decadepsipeptides **24–26** lacking both chromophores and was extended to provide **32** lacking one of the two chromophores. The characterization of the DNA-binding properties of sandramycin vs **25** and **32** is detailed. The largest share of the binding is derived from the cyclic decadepsipeptide ($\Delta G^\circ = -6.0$ kcal/mol) and the incremental addition of each chromophore increases the binding approximately 3.2 and 1.0 kcal/mol, respectively. This is consistent with the representation of sandramycin and the luzopeptins as minor groove binding cyclic decadepsipeptides incrementally stabilized by mono and bisintercalation. Following the same trends, sandramycin and luzopeptin A were found to be nearly equivalent, exceptionally potent cytotoxic agents (6–0.02 nM), 500–1000 \times more potent than the cyclic decadepsipeptide **32** possessing a single chromophore, and $\geq 10^5 \times$ more potent than the cyclic decadepsipeptides **24** and **25** lacking both chromophores. DNase I footprinting studies revealed that sandramycin and luzopeptin A behave comparably and appear to bind best to regions containing alternating A and T residues. Binding at other and perhaps all sites is observed at modest agent concentrations with a perceptible preference for 5'-AT dinucleotide sequences many of which were preceded by a 5'-C, *i.e.* 5'-CAT. Preliminary studies of the 1:1 complex of sandramycin with 5'-d(GCATGC)₂ revealed that it maintains the 2-fold axis of symmetry of the components with the agent sandwiching the central two AT base pairs and adopting a compact conformation in which the interchromophore distance is 10.1 Å. The cyclic decadepsipeptide is positioned in the minor groove and the adopted conformation permits a rich array of complementary hydrophobic contacts extending over much of the interacting surface.

Sandramycin (**1**), a potent antitumor antibiotic¹ isolated from the culture broth of a *Norcardioides* sp. (ATCC 39419) and structurally characterized through extensive spectroscopic and chemical degradation studies,² constitutes one of the newest members of a growing class of cyclic decadepsipeptides including luzopeptins A–C, E₂,³ and quinaldopeptin⁴ which possess potent antitumor, antiviral, and antimicrobial activity.^{3–5} Characteristic of this class of agents, sandramycin possesses a 2-fold axis of symmetry and two pendant heteroaromatic chromophores that could be anticipated to result in DNA bifunctional intercalation similar to that detailed for the luzopeptins which span two base pairs preferentially at 5'-AT sites.^{6–8} In this respect, the agents are functionally related to echinomycin and triostin A, bicyclic octadepsipeptides, which

also bind to DNA by bisintercalation but with a different sequence selectivity (5'-CG versus 5'-AT).^{9–11}

Herein, we provide full details of the total synthesis of (–)-sandramycin (**1**) which constitutes the first total synthesis^{12,13} of a naturally occurring member of this class of agents and that served to confirm the structural and absolute stereochemical assignments of **1**. Key strategic elements of the approach

(6) (a) Fox, K. R.; Woolley, C. *Biochem. Pharmacol.* **1990**, *39*, 941. (b) Fox, K. R.; Davies, H.; Adams, G. R.; Portugal, J.; Waring, M. J. *Nucleic Acids Res.* **1988**, *16*, 2489.

(7) Huang, C.-H.; Mong, S.; Crooke, S. T. *Biochemistry* **1980**, *19*, 5537. Huang, C.-H.; Prestayko, A. W.; Crooke, S. T. *Biochemistry* **1982**, *21*, 3704. Huang, C.-H.; Crooke, S. T. *Cancer Res.* **1985**, *45*, 3768. Huang, C.-H.; Mirabelli, C. K.; Mong, S.; Crooke, S. T. *Cancer Res.* **1983**, *43*, 2718.

(8) Leroy, J. L.; Gao, X.; Misra, V.; Gueron, M.; Patel, D. J. *Biochemistry* **1992**, *31*, 1407. Zhang, X.; Patel, D. J. *Biochemistry* **1991**, *30*, 4026. Searle, M. S.; Hall, J. G.; Denny, W. A.; Wakelin, L. P. G. *Biochem. J.* **1989**, *259*, 433.

(9) Waring, M. J.; Fox, K. R. In *Mol. Aspects of Anticancer Drug Action*; Waring, M. J., Neidle, S., Eds.; Verlag: Weinheim, 1983; p 127. UK-63052 and related agents: Rance, M. J.; Ruddock, J. C.; Pacey, M. S.; Cullen, W. P.; Huang, L. H.; Jefferson, M. T.; Whipple, E. B.; Maeda, H.; Tone, J. J. *Antibiot.* **1989**, *42*, 206. Fox, K. R. *J. Antibiot.* **1990**, *43*, 1307.

(10) Wang, A. H.-J.; Ughetto, G.; Quigley, G. J.; Hakoshima, T.; van der Marel, G. A.; van Boom, J. H.; Rich, A. *Science* **1984**, *225*, 1115. Ughetto, G.; Wang, A. H.-J.; Quigley, G. J.; van der Marel, G. A.; van Boom, J. H.; Rich, A. *Nucleic Acids Res.* **1985**, *13*, 2305. Van Dyke, M. M.; Dervan, P. B. *Science* **1984**, *225*, 1122.

(11) Synthesis: Chakravarty, P. K.; Olsen, R. K. *Tetrahedron Lett.* **1978**, *19*, 1613. Shin, M.; Inouye, K.; Otsuka, H. *Bull. Chem. Soc. Jpn.* **1984**, *57*, 2203. Ciardelli, T. L.; Chakravarty, P. K.; Olsen, R. K. *J. Am. Chem. Soc.* **1978**, *100*, 7684. Shin, M.; Inouye, K.; Higuchi, N.; Kyogoku, Y. *Bull. Chem. Soc. Jpn.* **1984**, *57*, 2211.

[⊗] Abstract published in *Advance ACS Abstracts*, January 15, 1996.

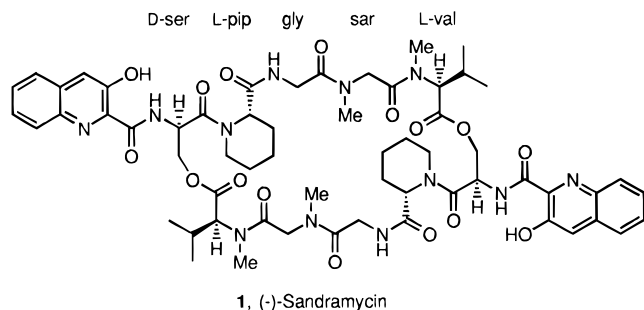
(1) Matson, J. A.; Bush, J. A. *J. Antibiot.* **1989**, *42*, 1763.

(2) Matson, J. A.; Colson, K. L.; Belofsky, G. N.; Bleiberg, B. B. *J. Antibiot.* **1993**, *46*, 162.

(3) (a) Ohkuma, H.; Sakai, F.; Nishiyama, Y.; Ohbayashi, M.; Imanishi, H.; Konishi, M.; Miyaki, T.; Koshiyama, H.; Kawaguchi, H. *J. Antibiot.* **1980**, *33*, 1087. Tomita, K.; Hoshino, Y.; Sasahira, T.; Kawaguchi, H. *J. Antibiot.* **1980**, *33*, 1098. Konishi, M.; Ohkuma, H.; Sakai, F.; Tsuno, T.; Koshiyama, H.; Naito, T.; Kawaguchi, H. *J. Antibiot.* **1981**, *34*, 148. (b) Konishi, M.; Ohkuma, H.; Sakai, F.; Tsuno, T.; Koshiyama, H.; Naito, T.; Kawaguchi, H. *J. Am. Chem. Soc.* **1981**, *103*, 1241. (c) Arnold, E.; Clardy, J. *J. Am. Chem. Soc.* **1981**, *103*, 1243.

(4) Toda, S.; Sugawara, K.; Nishiyama, Y.; Ohbayashi, M.; Ohkuma, N.; Yamamoto, H.; Konishi, M.; Oki, T. *J. Antibiot.* **1990**, *43*, 796.

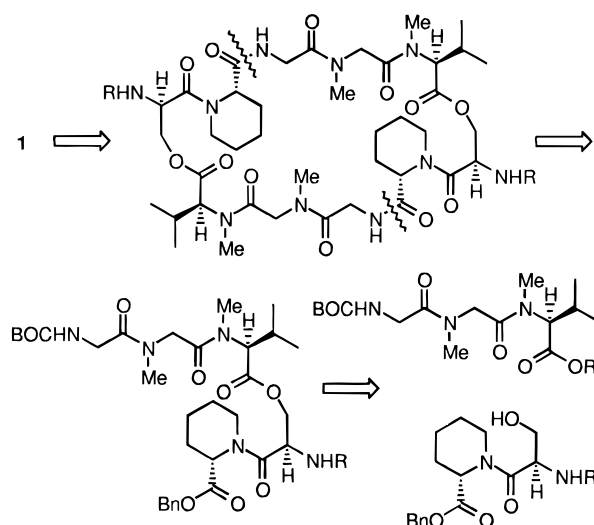
(5) Take, Y.; Inouye, Y.; Nakamura, S.; Allaldeen, H. S.; Kubo, A. *J. Antibiot.* **1989**, *42*, 107.



include the deliberate late stage introduction of the heteroaromatic chromophore thereby providing simple access to structural analogs possessing modified intercalation capabilities, symmetrical pentadepsipeptide coupling and macrocyclization of the 32-membered decadepsipeptide conducted at the single secondary amide site, and a convergent assemblage of the precursor pentadepsipeptide in which the potentially labile ester linkage was introduced in the final key coupling reaction (Scheme 1). The characterization of the high affinity, bifunctional intercalation of **1** is disclosed.

Pentadepsipeptide Synthesis. Coupling of BOC-Gly-Sar-OH (**3**)¹⁴ with L-NMe-Val-OCH₃¹⁵ (**5**, 1 equiv of DCC, 1.05 equiv of Et₃N, 0.1 equiv of DMAP, CH₂Cl₂, 25 °C, 24 h, 74%) followed by methyl ester hydrolysis of **6** (3 equiv of LiOH, 3:1:1 THF-CH₃OH-H₂O, 25 °C, 3 h, 90%) provided **7** and a key subunit for incorporation into the pentadepsipeptide **15** (Scheme 2). Coupling of L-pipecolic acid benzyl ester (**11**) prepared as illustrated in Scheme 2 from L-pipecolic acid¹⁶ with D-N-SES-Ser-OH (**13**, 1.3–1.4 equiv of BOP-Cl,¹⁷ 2.6–3.0 equiv of Et₃N or *i*-Pr₂NEt, CH₂Cl₂, 0 °C, 10 h, 82–85%) provided the dipeptide **14**. Notably, this coupling to provide a tertiary amide could be conducted without deliberate protection of the D-serine hydroxyl group, competitive racemization,¹⁷ or β-elimination and provided **14** in excellent yield suitably protected for direct incorporation into **15**. Moreover, the [β-(trimethylsilyl)ethyl]sulfonyl (SES) group¹⁸ incorporated into **14–15** served as an admirable orthogonal peptide protecting group stable to BOC and benzyl ester deprotection yet capable of selective removal in the presence of the depsipeptide ester. However, this coupling of the secondary amine of a pipecolic acid derivative proved more challenging than the results described above might suggest. A wide range of amide coupling procedures were examined and provided modest results analogous to the related observations of others.¹⁹ Attempts to promote the coupling with EDCI-HOBt under a range of reaction conditions (–30 to 25 °C, 12–48 h) with added bases (NaHCO₃, Et₃N, *i*-Pr₂NEt) in a range of reaction solvents (DMF, THF, CH₂Cl₂) provided **14** in modest conversions (20–40%)

Scheme 1



as did DCC-HOBt and DCC-DMAP (CH₂Cl₂, 25 °C, 24 h, 42%). Other carboxylate activation procedures including the use of *N*-methyl-2-chloropyridinium iodide,²⁰ a pivoyl mixed anhydride (toluene, 60 °C, 12 h, 19%),²¹ or DPPA²² (1.8 equiv, DMF, 25 °C, 20 h, 20–40%) were less successful. Attempts to employ *O*-silyl or *O*-benzyl derivatives of *N*-SES-D-Ser did not improve these observations and suggested that the problematic feature was not competitive reaction of the D-serine hydroxyl but rather the sluggish reaction of the benzyl L-pipecolate secondary amine.

Esterification of **7** with **14** provided the pentadepsipeptide **15** and was accomplished through use of DCC-DMAP²³ (1 equiv of DCC, 1.0 equiv of DMAP, CH₂Cl₂, 0 °C, 24 h, 79–89%). This esterification was anticipated to be problematic since the carboxylic acid coupling partner contains a *N*-methyl amide which is known to decelerate or preclude sensitive esterifications and increase the propensity for racemization and this is especially true of a sensitive *N*-methyl-L-valine center.²⁴ Moreover, the product sensitivity to subsequent β-elimination further restricted the choice of acylation conditions. Nonetheless, the coupling proved remarkably straightforward with the exception that racemization did prove problematic. Competitive racemization of the L-valine center was observed if the reaction was conducted under conventional conditions employing catalytic DMAP but the use of increasing amounts of DMAP was found to suppress epimerization (Table 1). Alternative esterification procedures including DCC-HOBt (1 equiv of DCC, 1.2 equiv of HOBt, DMF, 0 °C, 20 h, 54%), BOP-Cl (1.1 equiv, 2.2 equiv of Et₃N, CH₂Cl₂, 0 °C, 24 h, 41%) proved less successful.

In initial efforts, the prospect that the racemization of the L-valine center might be occurring during the conversion of **6** to provide **7** was also a concern especially because of the propensity for *N*-methyl amino acids to racemize during basic hydrolysis.²⁴ Consequently, BOC-NMe-L-Val-OBn (**18**)²⁵ was

(12) Boger, D. L.; Chen, J.-H. *J. Am. Chem. Soc.* **1993**, *115*, 11624.

(13) Olsen, R. K.; Apparao, S.; Bhat, K. L. *J. Org. Chem.* **1986**, *51*, 3079. Ciufolini, M. A.; Swaminathan, S. *Tetrahedron Lett.* **1989**, *30*, 3027. Hughes, P.; Clardy, J. *J. Org. Chem.* **1989**, *54*, 3260. Ciufolini, M. A.; Xi, N. *J. Chem. Soc., Chem. Commun.* **1994**, 1867. Greck, C.; Bischoff, L.; Genet, J. P. *Tetrahedron: Asymmetry* **1995**, *6*, 1989.

(14) Seebach, D.; Bossler, H.; Gründler, H.; Shoda, S.; Wenger, R. *Helv. Chim. Acta* **1991**, *74*, 197.

(15) *N*-BOC-NMe-Val-OCH₃ was prepared in one step from *N*-BOC-Val by exhaustive methylation (2.5–3 equiv of NaH, 8 equiv of CH₃I, 10:1 THF-DMF, reflux, 12–24 h, 78%) following the procedure of Coggins and Benoiton: Coggins, J. R.; Benoiton, N. L. *Can. J. Chem.* **1971**, *49*, 1968.

(16) L-Pipecolic acid benzyl ester was prepared from the L-pipecolic acid D-tartrate salt obtained by recrystallization and resolution (EtOH-H₂O, 3×, 71%); [α]_D²³ –20 (c 10, H₂O), lit. [α]_D²⁵ –20.2 (c 10, H₂O); Rodwell, V. W. *Methods Enzymol.* **1971**, *17*, Part B, 174.

(17) Tung, R. D.; Rich, D. H. *J. Am. Chem. Soc.* **1985**, *107*, 4342.

(18) Weinreb, S. M.; Demko, D. M.; Lessen, T. A. *Tetrahedron Lett.* **1986**, *27*, 2099.

(19) Perlow, D. S.; Erb, J. M.; Gould, N. P.; Tung, R. D.; Freidinger, R. M.; Williams, P. D.; Veber, D. F. *J. Org. Chem.* **1992**, *57*, 4394.

(20) Bald, E.; Saigo, K.; Mukaiyama, T. *Chem. Lett.* **1975**, 1163.

(21) Schreiber, S. L.; Anthony, N. J.; Dorsey, B. D.; Hawley, R. C. *Tetrahedron Lett.* **1988**, *29*, 6577 and references cited therein.

(22) Shioiri, T.; Yamada, S. *Chem. Pharm. Bull.* **1974**, *22*, 849. Kitada, C.; Fujino, C. *Chem. Pharm. Bull.* **1978**, *26*, 585.

(23) Hassner, A.; Alexanian, V. *Tetrahedron Lett.* **1978**, *19*, 4475.

(24) McDermott, J. R.; Benoiton, N. L. *Can. J. Chem.* **1973**, *51*, 2555. McDermott, J. R.; Benoiton, N. L. *Can. J. Chem.* **1973**, *51*, 2562. Ciardelli, T. L.; Chakravarty, P. K.; Olsen, R. K. *J. Am. Chem. Soc.* **1978**, *110*, 7684. Tung, R. D.; Dhaon, M. K.; Rich, D. H. *J. Org. Chem.* **1986**, *51*, 3350. Dhaon, M. K.; Olsen, R. K.; Ramasamy, K. J. *Org. Chem.* **1982**, *47*, 1962. Zegaf, C.; Poncet, J.; Jouin, P.; Dufour, M.-N.; Castro, B. *Tetrahedron* **1989**, *45*, 5039. Coste, J.; Frérot, E.; Jouin, P.; Castro, B. *Tetrahedron Lett.* **1991**, *32*, 1967.

Scheme 2

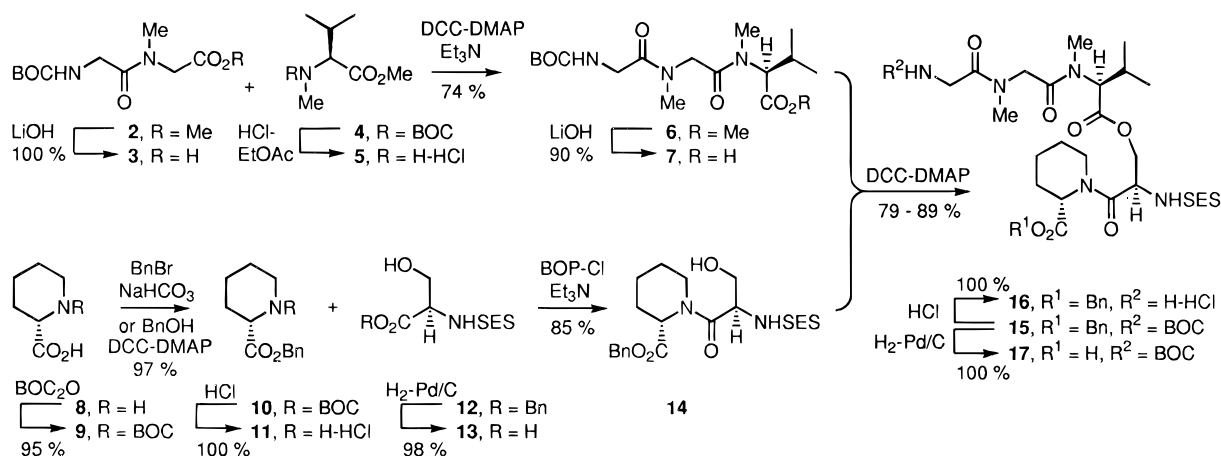
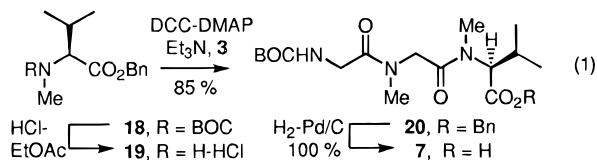


Table 1. Pentadepsipeptide 15 Synthesis

DMAP, equiv	% yield 15	epi-15
0.1	50	32
0.15	59	27
0.2	63	24
0.5	65	11
1.0	79-89	2-8

incorporated into the tripeptide **7** by coupling **19** with **3** (1.0 equiv of DCC, 0.5 equiv of DMAP, 1.1 equiv of Et₃N, CH₂-Cl₂, 25 °C, 24 h, 85%). Deprotection of **20** by catalytic hydrogenolysis (H₂, cat 10% Pd-C, CH₃OH, 25 °C, 12 h, 100%) cleanly provided **7** free of concerns of racemization of the L-valine center (eq 1). The use of material prepared in this



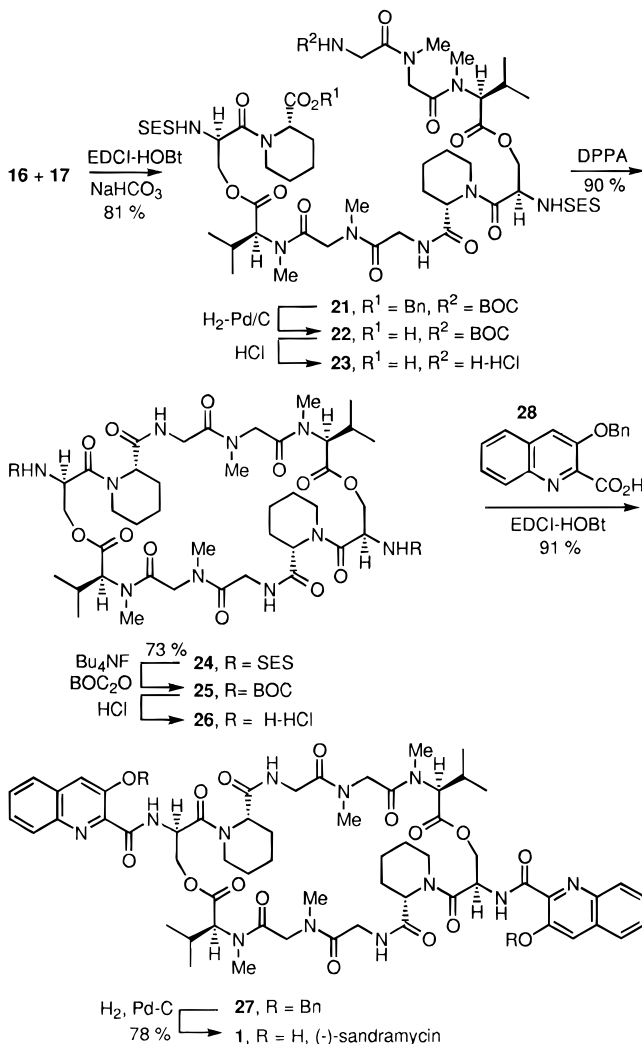
manner provided results comparable but perceptibly better than those obtained from the methyl ester **6**. The minor extent of racemization obtained in the esterification coupling of **7** with **14** in the presence of 1.0 equiv of DMAP was further diminished (2-6%) with the material derived from **20**, indicating that racemization also accompanies the hydrolysis of the methyl ester **6**. Thus, the approach detailed in eq 1 proceeding through **20** was adopted for our studies. Fortunately, the major (79-89%) and minor diastereomers (2-8%) were readily separable (SiO₂, R_f = 0.44 and 0.35, 67% EtOAc-hexane) and stereochemically homogeneous material was employed in the preparation of **1**.

Similarly, concerns arose in initial studies as to whether the benzyl L-pipecolate center had racemized under the conditions required for coupling of **11** with **13**. Consequently, racemic **11** was coupled with *N*-SES-D-Ser (**13**) and a distinguishable pair of resulting diastereomers was obtained. Their comparison with authentic **14** ensured that no detectable racemization of the L-pipecolic acid subunit had occurred. In addition, the sample of **14** containing the 1:1 mixture of D- and L-pipecolic acid was coupled with **7** and the resulting diastereomeric mixture of products **15** was not the same mixture of products obtained above indicating that the racemization encountered could be attributed to the NMe-Val center.

Cyclic Decadepsipeptide Formation and Completion of the Total Synthesis of (-)-Sandramycin (1). Linear decadep-

(25) *N*-BOC-NMe-Val-OBn was prepared by *N*-methylation of *N*-BOC-Val-OBn (1.5 equiv of NaH, 4.2 equiv of CH₃I, 10:1 THF-DMF, reflux, 24 h, 90%). For **18**: Wenger, R. M. *Helv. Chim. Acta* **1983**, *66*, 2672.

Scheme 3

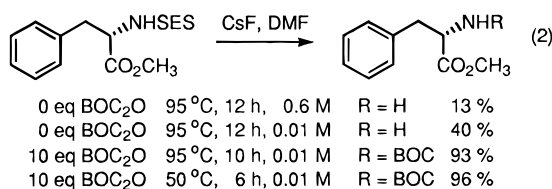


sipeptide formation was accomplished by independent deprotection of the amine (3 M HCl-EtOAc, 25 °C, 30 min, 100%) and carboxylic acid terminus (H₂, 10% Pd-C, CH₃OH, 25 °C, 12 h, 98%) of **15** to provide **16** and **17**, respectively, which were coupled with formation of the single secondary amide (1 equiv of EDCI, 1 equiv of HOBT, 4.0 equiv of NaHCO₃, CH₂-Cl₂, 25 °C, 24 h, 81%) to provide **21** in excellent conversion (Scheme 3). This same coupling reaction conducted with Et₃N (2.0 equiv) in place of NaHCO₃ provided **21** in substantially lower conversions (55%) and may reflect the sensitivity of the

pentadecapeptides **16** and **17** or the product decadepsipeptide to base-catalyzed β -elimination.

Cyclization of **21** to provide the 32-membered cyclic decadepsipeptide **24**, $[\alpha]_D^{23} -88$ (c 0.85, CHCl_3), with the ring closure strategically conducted at the single secondary amide site was accomplished in superb conversion by sequential benzyl ester (H_2 , 10% Pd-C, CH_3OH , 25 °C, 12 h) and BOC deprotection (3 M HCl-EtOAc, 25 °C, 30 min) followed by treatment of **23** with diphenyl phosphorazidate (4 equiv of DPPA, 10 equiv of NaHCO_3 , 0.003 M DMF, 0 °C, 48 h, 90% overall).²⁶ Upon cyclization, the cyclic decadepsipeptide adopts a single rigid solution conformation comparable to that observed with **1**. Given the facility of the 32-membered ring macrocyclization reaction, we also attempted to simply couple the pentapeptides and effect the ring closure in a single reaction. However, hydrogenolysis of the benzyl ester **15**, acid-catalyzed deprotection of the resulting **17** (3 M HCl-EtOAc, 25 °C, 30 min, 100%) and treatment of the product amino acid with DPPA (4 equiv, 10 equiv of NaHCO_3 , 0.01 M DMF, 0 °C, 48 h) provided only small amounts of **24** along with a full range of oligomers and higher order macrocycles.

Removal of the SES amine protecting group was accomplished under mild conditions (10 equiv of Bu_4NF , 22–30 equiv of BOC_2O , THF, 25 °C, 48 h, 70–73%) but required in situ trap of the liberated amine as its BOC derivative **25**, $[\alpha]_D^{23} -53$ (c 0.15, CHCl_3), for isolation. Presumably this may be attributed to the instability of the linking ester in the decadepsipeptide to the liberated amine under the anhydrous and basic reaction conditions. However, this deprotection was accomplished under surprisingly mild reaction conditions (25 °C). Since SES amine deprotections generally required higher reaction temperatures (50–100 °C), we cannot rule out the possibility that BOC acylation of the amine precedes and activates the subsequent SES deprotection. Although this was not investigated in detail, initial efforts to check our reagents (CsF or Bu_4NF) with the simple substrate *N*-SES-Phe-OCH₃ provided only low conversions to the expected free amine and afforded substantial or predominant amounts of the corresponding diketopiperazine (eq 2). Conducting this deprotection with



CsF or Bu_4NF in the presence of BOC_2O (10 equiv) cleanly provided *N*-BOC-Phe-OCH₃ and this protocol may serve as an excellent solution for those who encounter similar difficulties.¹⁸

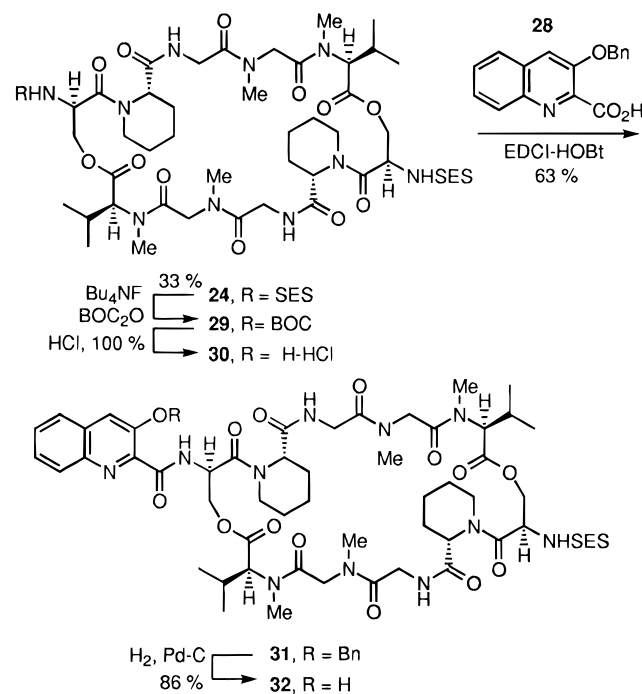
A single-crystal X-ray structure determination of **25**²⁷ confirmed the structural and stereochemical assignments and further revealed a rigid cyclic decadepsipeptide conformation essentially identical to that found in the X-ray structure of luzopeptin A.^{3c} Completion of the synthesis required BOC deprotection of **25** (3 M HCl-EtOAc, 25 °C, 30 min), coupling of the resulting bis amine **26** with 3-(benzyloxy)quinoline-2-carboxylic acid (**28**,²⁸ 4.0 equiv of EDCI, 6.0 equiv of HOBT, 10 equiv of NaHCO_3 , DMF, 25 °C, 72 h, 91%) and a final deprotection of bis-*O*-benzylsandracycin (**27**, $[\alpha]_D^{23} -107$ (c 0.3, CHCl_3); H_2 ,

(26) Brady, S. F.; Freidinger, R. M.; Paleveda, W. J.; Colton, C. D.; Homnick, C. F.; Whitter, W. L.; Curley, P.; Nutt, R. F.; Veber, D. F. *J. Org. Chem.* **1987**, *52*, 764.

(27) The author has deposited the atomic coordinates for this structure with the Cambridge Crystallographic Data Centre. The coordinates may be obtained upon request from the Director, Cambridge Crystallographic Data Centre, 12 Union Road, Cambridge, CB2, 1EZ, UK.

(28) Boger, D. L.; Chen, J.-H. *J. Org. Chem.* **1995**, *60*, 7369.

Scheme 4



10% Pd-C, EtOAc, 25 °C, 12 h, 78%) to provide (–)-**1**, $[\alpha]_D^{23} -153$ (c 0.17, CHCl_3), which was identical in all respects with a sample of authentic material (¹H NMR, ¹³C NMR, IR, MS, UV, mp, $[\alpha]_D$, and chromatographic properties).

Preparation of Cyclic Decadepsipeptide 32 Possessing a Single Chromophore. For comparisons with **1** and the agents **24–26** lacking both of the chromophores, the agent **32** possessing a single chromophore was also prepared. In initial studies on the deprotection of **24**, exposure to Bu_4NF (4 equiv) for shorter periods of time (24 h, 25 °C) in the presence of BOC_2O (10 equiv) led to partial deprotection to provide **29** (33%) along with recovered **24** (11%) and **25** (27%) (Scheme 4). Without further attempts at optimization, this inadvertent preparation of **29** provided sufficient material for our synthesis of **32**. Acid-catalyzed BOC deprotection of **29** (3 M HCl-EtOAc, 25 °C, 30 min) followed by acylation of the liberated amine hydrochloride salt **30** with **28** (4 equiv of EDCI, 6 equiv of HOBT, 10 equiv of NaHCO_3 , 25 °C, 48 h, 63%) and subsequent catalytic hydrogenolysis of the benzyl ether **31** (H_2 , cat. 10% Pd-C, EtOAc, 25 °C, 14 h, 86%) cleanly provided **32**, $[\alpha]_D^{25} -105$ (c 0.3, CHCl_3).

Conformational Properties of 1 and the Related Cyclic Decadepsipeptide 25. The X-ray structure determination of **25**²⁷ revealed a backbone conformation nearly identical to that of luzopeptin A (Figure 1, rms = 1.40 Å).^{3c} The most significant difference in the two structures is the twisted orientation of the linking esters. The relative placement of the ring nitrogens (rms = 0.73 Å) and the backbone conformation of the pentapeptides excluding the ester atoms (rms = 0.74 Å) are even more similar in the two structures. The overall shape of the agent is rectangular with a 2-fold axis of symmetry. The long sides of the rectangle consist of antiparallel and twisted β -extended chains capped on either end by the two decadepsipeptide ester linkages. Each of the amides including the three tertiary amides adopt a trans or extended stereochemistry and the two decadepsipeptide esters adopt the preferred syn conformation. The two symmetrical glycine secondary amide NH's are engaged in tight transannular H-bonds (2.08 Å, gly-NH–O=C–gly) to the glycine carbonyl oxygen across the ring and cap two reverse peptide turns induced in part by the incorporation of unnatural D-serine at one corner of each turn.

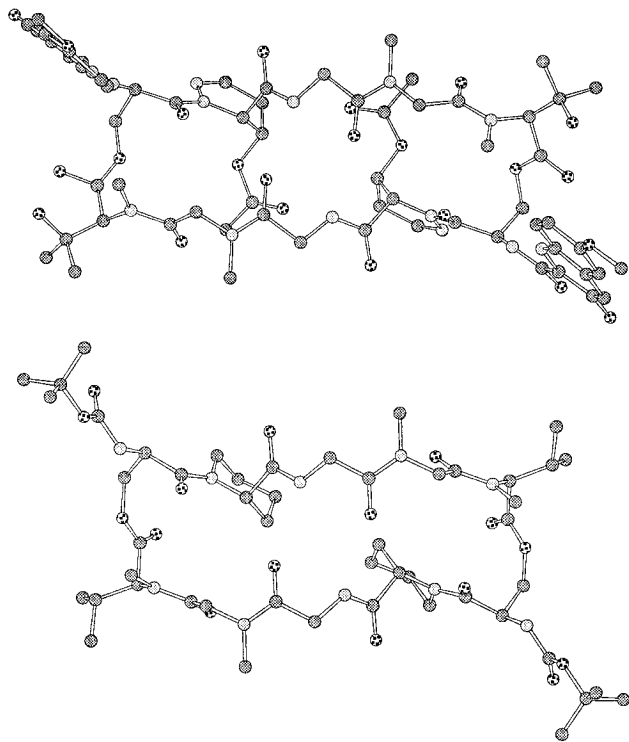


Figure 1. ChemDraw 3D representations of the X-ray structures of luzopeptin A^{3c} (top) and **25** (bottom).

Table 2. ¹H NMR (400 MHz) of **25**

proton		δ	
		25 , CDCl ₃	sandramycin, CDCl ₃
Gly-NH	2H	8.46 (d, 5.2)	8.52 (d, 4.4)
Boc-NH	2H	5.85 (d, 6.1)	
Sar- α -CH	2H	5.35 (d, 16.8)	5.54 (d, 16.6)
Pip- α -CH	2H	5.28 (d, 4.8)	5.57 (d, 6.4)
Ser- α -CH	2H	4.82 (d, 6.1)	5.26 (d, 5.0)
Val- α -CH	2H	4.80 (d, 11.0)	4.87 (d, 11.0)
Ser- β -CH ₂	4H	4.47 (s)	4.99 (d, 11.7)
			4.43 (d, 11.7)
Gly- α -CH	2H	4.41 (dd, 18.0, 5.2)	4.43 (d, 11.7)
Gly- α -CH	2H	4.03 (d, 18.0)	4.06 (m)
Pip- ϵ -CH (ax)	2H	3.90 (app t, 12.0)	4.10 (m)
Pip- ϵ -CH (eq)	2H	3.61 (d, 12.0)	3.74 (d, 14.5)
Sar- α -CH	2H	3.42 (d, 16.8)	3.55 (d, 16.6)
Val-NCH ₃	6H	2.95 (s)	3.12 (s)
Sar-NCH ₃	6H	2.92 (s)	2.94 (s)
Val- β -CH	2H	2.13 (dsp, 11.0, 6.5)	2.04 (dsp, 11.0, 6.4)
Pip-(CH ₂) ₃	12H	1.65 (m)	1.73 (m), 1.59 (m), 1.47 (m)
Boc	18H	1.40 (s)	
Val- γ -CH ₃	6H	0.98 (d, 6.5)	0.92 (d, 6.4)
Val- γ -CH ₃	6H	0.84 (d, 6.5)	0.78 (d, 6.4)

The pipecolic acid residue adopts a chair conformation with the α -carboxylate adopting an axial position and skewed by approximately 48° from the optimal carbonyl/C α -H anti relationship. In this conformation the D-ser-NH/D-ser-NH distance is 15.1 Å. The comparable luzopeptin A D-ser-NH/D-ser-NH distance is 14.8 Å and the distance between the centers of the two chromophores in this X-ray is 17.4–19.9 Å.

The 1D ¹H NMR of **24** and **25** indicate that they adopt a single, rigid solution conformation comparable to that observed with sandramycin. Consequently, **25** was examined in detail. Complete proton assignments in the ¹H NMR of **25** (Table 2) were made by both ¹H–¹H COSY and 1D ¹H NMR decoupling experiments in a range of solvents (CDCl₃, THF-*d*₈, CD₃OD, DMF-*d*₇, DMSO-*d*₆, supporting information) and confirmed by ¹H–¹H NOESY and ROESY NMR experiments (Table 3). The ROESY spectrum was used to distinguish intermolecular NOE

and exchange peaks. In all solvents except DMSO-*d*₆, the agent **25** adopted a single, rigid solution conformation comparable to that observed in the X-ray and comparable to that observed with **1** itself (Figure 6, supporting information). In DMSO-*d*₆, the ¹H NMR spectrum was broad and nondescript, indicating multiple conformations with no single one dominating although the conformation adopted in other solvents was observable. Clear from these studies, the agent **25** as well as **1** adopt a single solution conformation in all solvents except DMSO-*d*₆ that is analogous to the X-ray conformation in which all amides including the three tertiary amides are trans.

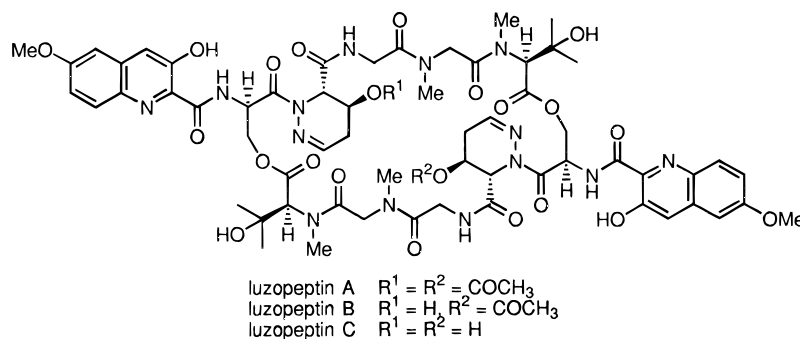
Several significant NOEs and diagnostic coupling constants were used to establish the stereochemistry of the amides, their orientation, and decadepsipeptide backbone conformation. The presence of pip- ϵ -CH(eq)/ser- α -CH and ser- β -CH₂ NOE crosspeaks established the trans D-ser-pip amide stereochemistry, the local orientation of the pip six-membered ring, and the presence of the D-ser turn. The absence of pip- ϵ -CH(ax)/ser- α -CH or ser- β -CH₂ NOEs further fixed these orientations analogous to that seen in the X-ray and the absence of a ser- α -CH/pip- α -CH NOE excluded the presence of a *cis*-ser-pip amide. A strong gly-NH/pip- α -CH NOE established their syn orientation comparable to that observed in the X-ray and the trans pip-gly amide bond. The equally intense and strong NOE crosspeaks between sar-NMe and both protons of gly- α -CH₂ indicated a *trans*-gly-sar *N*-methyl amide stereochemistry. Moreover, the two protons of gly- α -CH₂ and gly-NH exhibit coupling constants of 5.2 and 0 Hz and are consistent with only two combinations of dihedral angles (–90 and 150° or 90 and –30°). The former corresponds to that observed in the X-ray with the gly-NH and gly carbonyl eclipsed and oriented for transannular H-bonding to the corresponding residue on the opposite side of the ring and is consistent with the observed weak gly-NH/gly- α -CH₂ NOE crosspeaks. The strong NOE to both protons of sar- α -CH₂/val-NMe are diagnostic of a *trans*-sar-NMe-val amide and served to establish their proximal orientations. Diagnostic of the twist in the extended sheet observed in the X-ray, one sar-NMe/sar- α -CH NOE was observed and one was not. A strong val-NMe/val- β -CH NOE was observed and is consistent with their syn orientation. Similarly, the pattern of NOEs for the val side-chain methyl groups and the large val- β -CH/val- α -CH coupling constant ($J = 11.1$ – 10.9 Hz) are consistent with a well-defined solution conformation analogous to that observed in the X-ray where the val- β -CH and val- α -CH are trans antiperiplanar to one another. The absence of a ser- β -CH₂/val-NMe NOE established the relative orientations of the sar-NMe-val amide and decadepsipeptide ester similar to that observed in the X-ray as do the absence of ser- β -CH₂/val- α -CH, β -CH or γ -CH₃ NOEs. The orientation of the BOC-NH-ser is fixed by the observance of a val-NMe/ser-NH NOE and by the absence of a ser-NH/ser- β -CH₂ NOEs.

The gly-NH exhibited a high chemical shift (δ 8.46–8.35) and no solvent dependence providing a clear indication that it is participating in a strong H-bond with the transannular gly carbonyl. In contrast, the D-ser-NH exhibited a much lower chemical shift of δ 5.09–6.53 and a much larger solvent dependence. Finally, the exchange rates for the D-ser-NH and gly-NH were measured in 5% D₂O in DMF-*d*₇. Consistent with this proposed H-bonding, the solvent accessible D-ser-NH exchanged rapidly ($t_{1/2} < 2$ min) while the H-bonding gly-NH exchanged much more slowly and required 9–10 h for complete exchange ($t_{1/2} = 1.5$ h).

Similar characteristics to those detailed above were observed with the solution conformation of **1** in both our studies and those detailed by Matson² and are consistent with the solution

Table 3. ^1H - ^1H NOEs Observed with **25** in CDCl_3

proton	δ ,	observed NOE to	δ	proton	δ ,	observed NOE to	δ
Gly-NH	8.46	Pip- α -CH	5.28	Pip- ϵ -CH (eq)	3.61	Ser- α -CH	4.82
		Gly- α -CH	4.41 (w)			Ser- β -CH ₂	4.47
		Gly- α -CH	4.03 (w)			Pip- ϵ -CH	3.90
Boc-NH	5.85	Ser- α -CH	4.82	Sar- α -CH ₂	3.42	Sar- α -CH	5.35
		Val-NCH ₃	2.95			Val-NCH ₃	2.95
Sar- α -CH	5.35	Sar- α -CH	3.42	Val-NCH ₃	2.95	Sar-NCH ₃	2.92
		Val-NCH ₃	2.95			Boc-NH	5.85 (w)
Pip- α -CH	5.28	Gly-NH	8.46	Sar- α -CH	5.35	Val- α -CH	4.80 (w)
		Ser- α -CH	4.82			Sar- α -CH	3.42
Ser- β -CH ₂	4.47	Boc-NH	5.85	Val- β -CH	2.13	Val- β -CH	2.13
		Ser- β -CH ₂	4.47			Val- β -CH	2.13
Val- α -CH	4.80	Pip- ϵ -CH	3.61	Boc-NH	1.40 (w)	Val- γ -CH ₃	0.84
		Val-NCH ₃	2.95 (w)			Val- γ -CH ₃	0.84
Val- β -CH	2.13 (w)	Val- β -CH	2.13 (w)	Sar-NCH ₃	2.92	Gly- α -CH	4.41
		Val- γ -CH ₃	0.98			Gly- α -CH	4.03
Val- γ -CH ₃	0.98	Val- γ -CH ₃	0.84	Val- β -CH	2.13	Sar- α -CH	3.42
		Sar- α -CH	4.82			Val- α -CH	4.80 (w)
Ser- α -CH	4.82	Pip- ϵ -CH	3.61	Val-NCH ₃	2.95	Val- γ -CH ₃	0.98 (w)
		Gly-NH	8.46 (w)			Val- γ -CH ₃	0.84 (w)
Gly- α -CH	4.41	Gly- α -CH	4.03	Boc	1.40	Val-NCH ₃	2.95 (w)
		Sar-NCH ₃	2.92			Val- α -CH	4.80
Gly- α -CH	4.03	Gly-NH	8.46 (w)	Val- β -CH	2.13	Val- β -CH	2.13
		Gly- α -CH	4.41			Val- α -CH	4.80
Sar-NCH ₃	2.92	Sar-NCH ₃	2.92	Val- α -CH	4.80	Val- α -CH	4.80
		Pip- ϵ -CH	3.61			Val-NCH ₃	2.95
Pip- ϵ -CH (ax)	3.90	Pip- ϵ -CH	3.61	Val- β -CH	2.13	Val- α -CH	4.80
						Val-NCH ₃	2.95
						Val- β -CH	2.13

Chart 1. Luzozeptin Structures

properties detailed previously for luzozeptin (Chart 1).²⁹ Analogous to studies conducted with luzozeptin,³⁰ the bisintercalation of **1** has been shown to span two base pairs and requires the adoption of a conformation in which the two chromophores are separated by 10.1–10.2 Å. However, the X-ray and related solution conformation of **1** consists of a more extended structure in which the interchromophore distance is 17–19.5 Å more consistent with bisintercalation spanning three base pairs. Consequently, we elected to examine the conformational properties of **1** and the related cyclic decapeptide under a variety of conditions. Since the conformation of cyclic peptides in water may be substantially different from that observed in nonpolar or aprotic solvents or in the solid state, we were interested in assessing the conformational properties of **1** or **25** in water as well. However, the solubility was much too low for such an evaluation and the progressive addition of D₂O to DMF-*d*₇ solutions of sandramycin (0–40%) or **25** did not result in perceptible alterations in the ^1H NMR spectrum or the detection of new or altered conformational states. Consequently, the ^1H NMR of **25** was examined in the presence of LiCl. The addition of lithium salts in THF has been shown to affect

solubility,³¹ promote deaggregation,³² and alter the conformational properties of peptides.^{33–37} Notably, the LiCl complexed cyclic peptides have been suggested to more accurately reflect the conformational properties in water and to do so by disrupting intramolecular hydrogen bonds necessarily adopted in nonpolar or aprotic solvents.

The progressive addition of LiCl (1–40 equiv) to **25** in THF-*d*₈ was examined by ^1H NMR. Additions of 1, 2, 5 or 10 equiv of LiCl to the solution resulted in surprisingly little change in the conformational properties of **25** with the original, still dominant conformation being observed and several (>3–4)

(31) Senn, H.; Loosli, H.-R.; Sanner, M.; Braun, W. *Biopolymers* **1990**, 29, 1387.

(32) Seebach, D.; Thaler, A.; Beck, A. K. *Helv. Chim. Acta* **1989**, 72, 857.

(33) Thaler, A.; Seebach, D.; Cardinaux, F. *Helv. Chim. Acta* **1991**, 74, 617, 628.

(34) Kessler, H.; Hehlein, W.; Schuck, R. *J. Am. Chem. Soc.* **1982**, 104, 4534.

(35) Kock, M.; Kessler, H.; Seebach, D.; Thaler, A. *J. Am. Chem. Soc.* **1992**, 114, 2676. Seebach, D.; Beck, A. K.; Bossler, H. G.; Gerber, C.; Ko, S. Y.; Murtiashaw, C. W.; Naef, R.; Shoda, S.; Thaler, A.; Krieger, M.; Wenger, R. *Helv. Chim. Acta* **1993**, 76, 1564. Seebach, D.; Bossler, H. G.; Flowers, R.; Arnett, E. M. *Helv. Chim. Acta* **1994**, 77, 291. Review: Seebach, D.; Beck, A. K.; Studer, A. In *Modern Synthetic Methods*; Ernst, B., Leumann, C., Eds.; VCH Publishers: Weinheim, 1995; pp 3–178.

(36) Kofron, J. L.; Kuzmic, P.; Kishore, V.; Gemmecker, G.; Fesik, S. W.; Rich, D. H. *J. Am. Chem. Soc.* **1992**, 114, 2670.

(37) Boger, D. L.; Patane, M. A.; Zhou, J. *J. Am. Chem. Soc.* **1995**, 117, 7357.

(29) Searle, M. S.; Hall, J. G.; Wakelin, L. P. G. *Biochem. J.* **1988**, 256, 271. Searle, M. S.; Hall, J. G.; Denny, W. A.; Wakelin, L. P. G. *Biochem. J.* **1989**, 259, 433. Frey, M.-H.; Leupin, W.; Sorensen, D. W.; Denny, W. A.; Ernst, R. R.; Wuthrich, K. *Biopolymers* **1985**, 24, 2371. Searle, M. S.; Hall, J. G.; Penny, W. A.; Wakelin, L. P. G. *Biochemistry* **1988**, 27, 4340.

(30) Zhang, X.; Patel, D. J. *Biochemistry* **1991**, 30, 4026.

Table 4. Comparative DNA Binding Properties

property	sandramycin (1)	luzopeptin A	32	25 ^b
$K_B,^a M^{-1}$	3.4×10^7 (1:6.7)	1.2×10^7 (1:4.5)	5.7×10^6 (1:4.8)	2.4×10^4
(-)-unwinding [c] ^c	0.022	0.044–0.11		
(+)-winding [c] ^d	0.044	0.22		

^a Calf thymus DNA, K_B = apparent absolute binding constant determined by fluorescence quenching. The value in parentheses is the agent/base pair ratio at saturating high-affinity binding and may be considered a measure of the selectivity of binding. ^b Determined indirectly by competitive binding with **1**. ^c Agent/base pair ratio required to unwind negatively supercoiled Φ X174 DNA (form I \rightarrow form II gel mobility, 0.9% agarose gel). ^d Agent/base pair ratio required to induce complete rewinding or positive supercoiling of Φ X174 DNA (form II \rightarrow form I gel mobility, 0.9% agarose gel).

trace conformational isomers (<5%) starting to appear. Notably, the gly-NH experienced no chemical shift change throughout the addition, indicating its maintained participation in a tight transannular H-bond while the D-ser-NH exhibited a more typical 0.4–0.5 ppm downfield chemical shift. Upon addition of 20–40 equiv of LiCl, the relative proportion of the dominant conformation diminished and at 40 equiv no unique or discrete conformations were identifiable. Thus, upon addition of LiCl to **1** no discrete set of new conformations could be identified and the agent appears to adopt a large number of additional accessible conformations.

As detailed in subsequent studies, sandramycin adopts a DNA-bound conformation that is substantially different than its native X-ray or solution conformation and this preferred conformation is inherent in the cyclic decadepsipeptides **24**–**26**. Only in DMSO or upon addition of LiCl (40 equiv) do multiple alternative conformations become apparent with **25**.

DNA Binding Affinity. Apparent absolute DNA binding constants and the apparent binding site sizes for **1**, luzopeptin A, and **32** were obtained by measurement of fluorescence quenching upon titration addition of calf thymus DNA.⁷ The excitation and emission spectra for sandramycin (**1**), luzopeptin A, and **32** in aqueous buffer were measured (Figure 7, supporting information) and, for the DNA binding assays which quantitate the fluorescence quenching, excitation outside the absorbance range of DNA was necessarily employed (360, 340, or 400 nm) and the more intense 530, 520, or 510 nm fluorescence emission monitored, respectively. For assay of the DNA-induced fluorescence quenching of the agents, a 2 mL buffer solution of Tris-HCl (pH 7.4) and 75 mM NaCl was employed. For titration, small aliquots of DNA were added to solutions of the agents in the Tris-HCl buffer (pH 7.4). The DNA quenching of fluorescence was nearly 70% with 360 nm excitation and 530 nm fluorescence for **1**, 60% with 340 nm excitation and 520 nm fluorescence for luzopeptin A, and 40% with 400 nm excitation and 510 nm fluorescence for **32**. The titrations were carried out with 5 min time intervals between DNA additions to allow binding equilibration. Notable differences have not been detected with different time intervals indicating that tight binding equilibration is rapid and the results are summarized in Table 4. The DNA titration fluorescence quenching was analyzed by Scatchard analysis³⁸ with the following equation: $r_b/c = Kn - Kr_b$ where r_b is the number of agent molecules bound per DNA nucleotide phosphate, c is the free drug concentration, K is the apparent association constant, and n is the number of agent binding sites per nucleotide phosphate. From a plot of r_b/c versus r_b as shown in Figure 2 for **1**, association constants (K_B) for **1**, luzopeptin A, and **32** were derived from the slopes and the binding site sizes determined from the intercept values (n) for the number

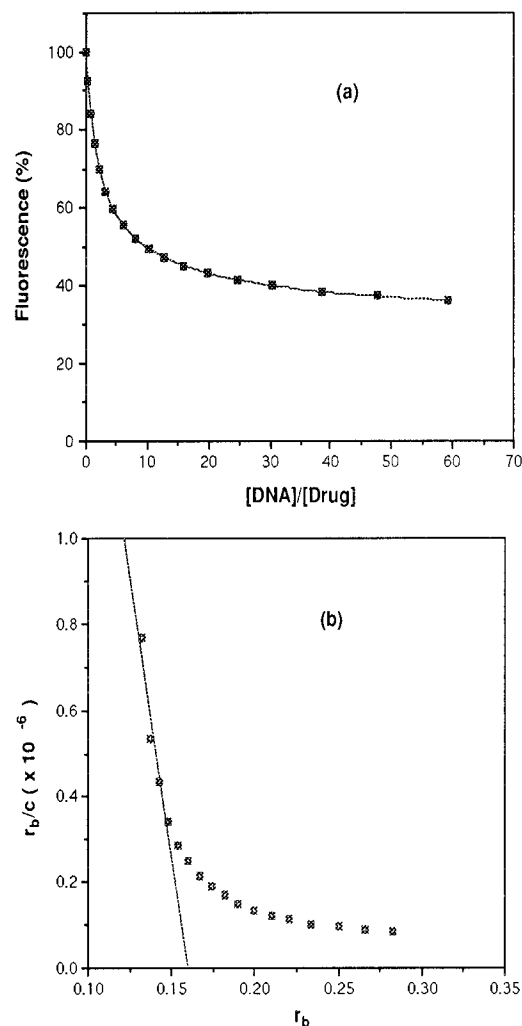


Figure 2. (a) Sandramycin fluorescence quenching at increasing calf thymus DNA concentrations, excitation at 360 nm, and emission at 530 nm in 10 mM Tris-HCl (pH 7.4) and 75 mM NaCl buffer solution, and (b) Scatchard plot of the fluorescence quenching of part a.

of binding sites per nucleotide phosphate. The results are summarized in Table 4.

The DNA binding constant for **25** could not be established by direct spectroscopic methods but was indirectly determined by two complementary and self consistent techniques. The first relied on competitive binding with **1** and inhibition of its DNA binding derived fluorescence quenching. This was accomplished by titrating small aliquots of **1** (1 mM in DMSO) into a solution of calf thymus DNA (320 μ M base pair) and **25** (320 μ M) in 10 mM Tris-HCl, 75 mM NaCl (pH 7.4) buffer. Scatchard plots of the titrations conducted in the presence or absence of various concentrations of **25** exhibited a well-defined competitive binding culminating in a common x intercept corresponding to the 1:6.7 agent/base pair ratio for saturated sandramycin binding. The second relied on the displacement of prebound ethidium bromide from calf thymus DNA and measurement of the resulting decrease in fluorescence.³⁹ Both methods provided comparable binding constants of $2.4 \times 10^4 M^{-1}$ and 4.0 – $8.0 \times 10^3 M^{-1}$, respectively. The titration of calf thymus DNA prebound with ethidium bromide relies on a determination of the amount of **25** required to displace one-half of the ethidium bromide established by a 50% fluorescence

(39) (a) Boger, D. L.; Invergo, B. J.; Coleman, R. S.; Zarrinmayeh, H.; Kitos, P. A.; Thompson, S. C.; Leong, T.; McLaughlin, L. W. *Chem.-Biol. Interact.* **1990**, *73*, 29. Boger, D. L.; Sakya, S. M. *J. Org. Chem.* **1992**, *57*, 1277. (b) Baguley, B. C.; Denny, W. A.; Atwell, G. J.; Cain, B. F. *J. Med. Chem.* **1981**, *24*, 170. For K_B of ethidium bromide: LePecq, J. B.; Paoletti, C. *J. Mol. Biol.* **1967**, *27*, 87.

reduction. This titration followed a well-defined linear reduction in fluorescence with added agent and provided comparable estimates of the K_B for **25** using either a competitive^{39b} ($4.0 \times 10^{-3} \text{ M}^{-1}$) or noncompetitive^{39a} ($8.0 \times 10^3 \text{ M}^{-1}$) binding model. Given the weak binding of **25**, these estimates are relatively insensitive to the stoichiometry of the displacement and binding site sizes of the agents. They are, however, subject to error if the binding of **25** does not preclude or compete with ethidium bromide binding. Unlike the observations actually made with **25**, such a nonideal behavior would also result in a nonlinear reduction in the ethidium bromide fluorescence, and the errors introduced by such nonideal behavior would lead to an underestimation of the apparent K_B . Thus, the K_B [$(4-8) \times 10^3 \text{ M}^{-1}$] established using this method may be best represented as the lower limit of the binding constant of **25** and, as such, agrees nicely with the results derived from the first method.

Sandramycin was found to exhibit an exceptionally high affinity for duplex DNA ($K_B = 3.4 \times 10^7 \text{ M}^{-1}$, $\Delta G^\circ = -10.2$ kcal/mol) with a saturating stoichiometry of high affinity binding at a 1:6.7 agent to base pair ratio. Notably, both the affinity and apparent selectivity is enhanced with **1** exhibiting saturated high affinity binding at a 1:6.7 agent/base pair ratio while that of luzopeptin A or **32** was observed at 1:4.5 and 1:4.8 agent/base pair ratios. The DNA binding constant of **1** proved to be slightly higher than that of luzopeptin A ($K_B = 1.2 \times 10^7 \text{ M}^{-1}$, $\Delta G^\circ = -9.6$ kcal/mol), substantially more effective than **32** ($K_B = 5.7 \times 10^6 \text{ M}^{-1}$, $\Delta G^\circ = -9.2$ kcal/mol) lacking one chromophore, and much more effective than **25** ($K_B = 2.4 \times 10^4 \text{ M}^{-1}$, $\Delta G^\circ = -6.0$ kcal/mol) lacking both chromophores. Importantly, the largest share of the binding affinity is derived from the cyclic decadepsipeptide and the addition of the first and second chromophores incrementally increase binding by approximately 3.2 and 1.0 kcal/mol, respectively. This is consistent with a representation of sandramycin and the luzopeptins as minor groove binding cyclic decadepsipeptides incrementally stabilized by mono and bisintercalation.

Bifunctional Intercalation. Confirmation that **1** binds to DNA with intercalation was derived from its ability to induce the unwinding of negatively supercoiled Φ X174 DNA.⁷ This was established by its ability to gradually decrease the agarose gel electrophoresis mobility of supercoiled Φ X174 DNA (unwinding) at increasing concentrations followed by a return to normal mobility (rewinding) at even higher agent concentrations. Similar types of changes have been reported for ethidium bromide under conditions which prevent dissociation of the bound agent during electrophoresis.⁴⁰

Under the conditions employed in our study, sandramycin completely unwound Φ X174 DNA at a 0.022 agent/base pair ratio and luzopeptin A at a 0.044–0.11 agent/base pair ratio (Figure 3, Table 4). Complete rewinding of the supercoiled DNA occurred at agent/base pair ratios of 0.044 and 0.22 for **1** and luzopeptin A, respectively. These comparisons along with the K_B measurements illustrate that sandramycin binds with either a higher unwinding angle or much slower offrate than luzopeptin A (unwinding angle = 43°).⁷

Similar evaluation of **32** lacking one of the two chromophores revealed a behavior analogous to ethidium bromide (Figure 3B). Under conditions where the monointercalator is not additionally present in the agarose gel, only a slight streaking and retardation of the electrophoretic mobility of the supercoiled Φ X174 DNA was observed. In comparable assays where ethidium bromide is present in the agarose gel which prevents its dissociation from DNA, ethidium bromide completely unwound supercoiled DNA at agent/base pair ratios of 0.090⁷ which is approximately 2–4 \times that required for **1** or luzopeptin A. Thus, the extent of

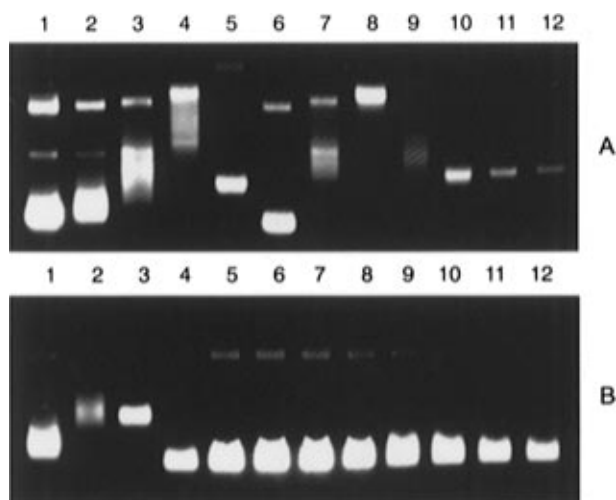


Figure 3. Agarose gel electrophoresis: (A) lanes 1–5, luzopeptin-A treated supercoiled Φ X174 RFI DNA; lane 6, untreated DNA, 95% form I and 5% form II; lanes 7–12 sandramycin-treated Φ X174 RFI DNA. The [agent] to [DNA] base pair ratios were 0.022 (lane 1), 0.033 (lane 2), 0.044 (lane 3), 0.11 (lane 4), 0.22 (lane 5), 0 (lane 6), 0.011 (lane 7), 0.022 (lane 8), 0.033 (lane 9), 0.044 (lane 10), 0.066 (lane 11), and 0.11 (lane 12). (B) Lanes 1–3, sandramycin-treated DNA; lane 4 untreated DNA, 95% form I and 5% form II; lanes 5–8, **32**-treated DNA; lanes 9–12, ethidium bromide-treated DNA. The [agent] to [DNA] base pair ratios were 0.011 (lane 1), 0.033 (lane 2), 0.066 (lane 3), 0 (lane 4), 0.87 (lane 5), 2.2 (lane 6), 5.0 (lane 7), 11.0 (lane 8), 0.87 (lane 9), 2.2 (lane 10), 5.0 (lane 11), 11.0 (lane 12).

unwinding of negatively supercoiled DNA and the subsequent positive supercoiling of the DNA by sandramycin, like luzopeptin A, was found to be indicative of bisintercalation while that of **32**, like ethidium bromide, was consistent with monointercalation.

DNA Binding Selectivity. DNase I⁴¹ and Fe^{II}-EDTA footprinting⁴² conducted following binding of sandramycin (**1**) and luzopeptin A to singly ³²P-end labeled w794 and w836 DNA⁴³ revealed that the agents behave comparably. Sandramycin more effectively protected DNA than luzopeptin A and more clearly revealed subtle distinctions in relative protection from DNA cleavage. Like the preceding studies with luzopeptin,⁶ sandramycin appears to bind best to regions containing alternating A and T residues, although no consensus di- or trinucleotide sequence was prominently detected. Binding at other sites is observed and at moderate agent concentrations the DNA is almost evenly protected from digestion. Illustrated in Figure 4 is the DNase I footprinting pattern obtained upon binding of sandramycin to w794 DNA. As indicated in Figure 4, the alteration of the DNase I digestion is barely perceptible at 2 μ M sandramycin, is evenly diminished at the higher agent concentrations of 10 and 20 μ M relative to controls. At these higher concentrations, some regions exhibit complete or near complete protection indicating preferential binding at these sites. Most, but not all such sites surround the dinucleotide sequence 5'-AT and most such sites are preceded by a 5'-C, *i.e.* 5'-CAT. The majority of the remaining sites are 5'-TA and both 5'-AT and 5'-TA appear to be preferred over 5'-AA or 5'-TT. However, these distinctions are subtle and most all sites are more evenly protected at even higher agent concentrations. The footprinting studies conducted with Fe^{II}-O₂ (HOCH₂CH₂SH) or Fe^{III}-H₂O₂ in the presence of EDTA provided comparable results but were more difficult to conduct with sufficient control to

(41) Galas, D. J.; Schmitz, A. *Nucleic Acids Res.* **1978**, *5*, 3157.

(42) Tullius, T. D.; Dombroski, B. A.; Churchill, M. E. A.; Kam, L. *Methods Enzymol.* **1987**, *155*, 537.

(43) Boger, D. L.; Munk, S. A.; Zarrinmayeh, H.; Ishizaki, T.; Haught, J.; Bina, M. *Tetrahedron* **1991**, *47*, 2661.

(40) Espejo, R. T.; Lebowitz, J. *Anal. Biochem.* **1976**, *72*, 95.

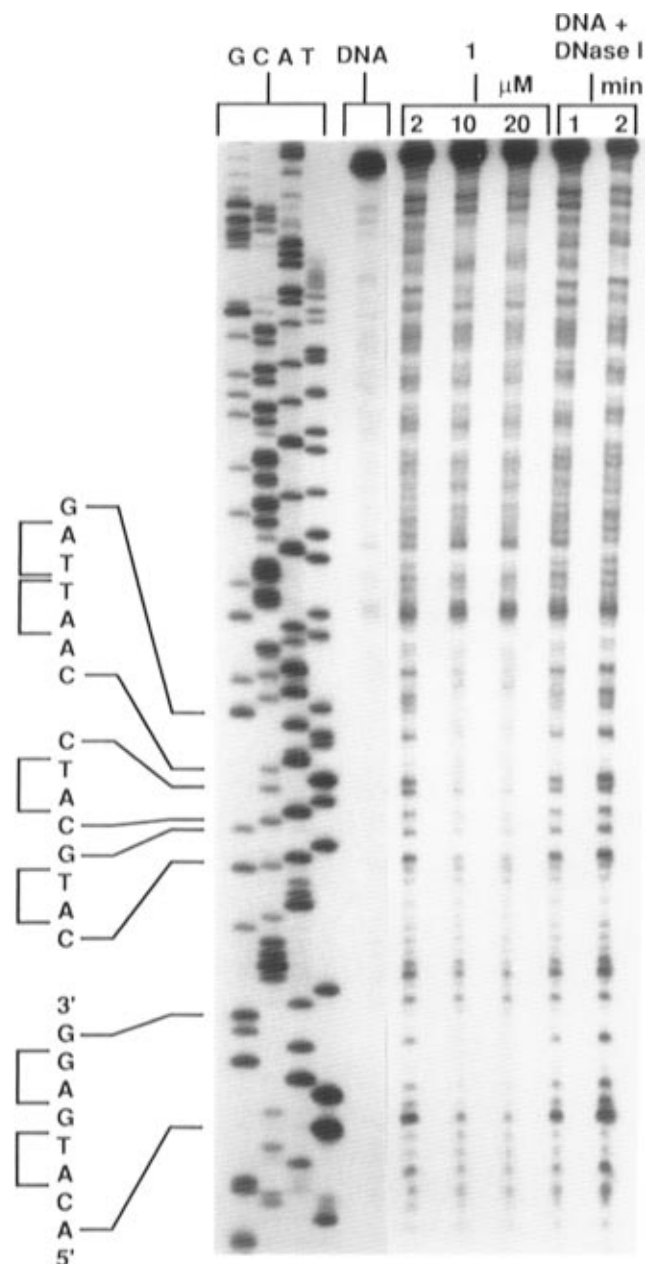


Figure 4. DNase footprinting of sandramycin (**1**) bound to w794 DNA. Lanes 1–4, G, C, A and T Sanger sequencing reactions; lane 5, control DNA; lanes 6–8, 2, 10, and 20 μM sandramycin with DNase I treatment (1 min); lanes 9 and 10, DNase I treatment of w794 DNA alone for 1 and 2 min.

detect the subtle selectivities. Under our conditions, little ligand induced enhancements of DNase I cleavage was observed in either GC or AT-rich regions although this was reported to be observed with the luzopeptins.⁶

Binding to 5'-d(GCATGC)₂. Similar to the results summarized above, prior footprinting studies with luzopeptin established that the agent binds best at regions containing alternating A-T base pairs although no consensus di- or trinucleotide sequence was established.⁶ Further studies of the luzopeptins with short DNA fragments (15–35 base pairs) indicated very strong incremental binding of the agent with saturated binding at about four base pairs per agent, implying it is capable of binding to all sequences with bisintercalation spanning two base pairs.⁶ Although the native X-ray structure and solution structures of **1**, luzopeptin, or the related cyclic decapeptides place the intercalating chromophores 17–19 Å apart and provides the potential for bisintercalation spanning three base pairs, recent NMR studies of luzopeptin

complexed with short deoxyoligonucleotides confirmed minor groove bisintercalation spanning two base pairs.^{8,29,30} Detailed NMR analysis of a luzopeptin complex with 5'-d(CATG)₂ has provided its solution structure with the agent sandwiching the central two Watson–Crick A-T base pairs and adopting a compact conformation in which the interchromophore distance is 10.1–10.2 Å.³⁰ Both the pip-gly secondary amides and the tertiary gly-sar amides adopt cis vs trans amide stereochemistries in order to accommodate this shortened distance and the agent maintains its 2-fold axis of symmetry. The gly-NH's are reoriented to form intermolecular H-bonds with the thymine C2 carbonyls and nicely explain the preference for the 5'-AT sequence.

In efforts which confirm this same binding mode for sandramycin (**1**), its 1:1 complex with 5'-d(GCATGC)₂²⁹ was prepared and examined in preliminary ¹H NMR studies.⁴⁴ Clear from the initial inspection of the 1D ¹H NMR was that complex formation had occurred cleanly to provide a symmetrical 1:1 complex. This rules out binding at one end of the oligo which would produce an unsymmetrical ¹H NMR pattern. Moreover, symmetrical binding in a 1:1 complex is restricted to bisintercalation spanning the central two or four base pairs and necessarily ruled out an unsymmetrical three base pair bisintercalation site. Since bisintercalation spanning four base pairs is structurally unrealistic, this also further restricts the bisintercalation to binding spanning the central two A-T base pairs of 5'-d(GCATGC)₂ analogous to the solution complexes observed with luzopeptin A bound to both 5'-d(GCATGC)₂ and 5'-d(CATG)₂.^{8,29,30}

The assignments for unbound **1** (Table 2), the free deoxyoligonucleotide²⁹ (Table 7, supporting information) and those for the complex were obtained from a combination of 1D and 2D ¹H NMR (Tables 7 and 8, supporting information) that identify connectivity and through-space interactions.⁴⁴ The position and orientation of the bound drug in the complex were revealed by perturbations in the ¹H NMR chemical shifts and intramolecular agent or oligonucleotide NOESY contacts and confirmed by several key intermolecular NOESY contacts. Characteristic of intercalation, all of the quinoline chromophore chemical shifts in the complex are shielded relative to those of the free agent (0.48–1.46 ppm) with the C7 and C8-H exhibiting the largest upfield shifts of 1.03 and 1.46 ppm, respectively. Further diagnostic of the intercalation site was the clear NOESY contacts between the quinoline C5-H and C6-H with the cytosine² C5-H and a complementary quinoline C7-H and adenine³ C8-H NOESY crosspeak. Not only does this identify the intercalation site but it also serves to orient the chromophore at the intercalation site and places the quinoline C4–C6 on the major groove interface and the chromophore C7, C8, and N1 on the minor groove side. These chemical shift perturbations and the location of the intermolecular contacts indicate that the chromophore carbocyclic ring stacks principally on the adenine base diagnostic of intercalation between the 5'-CpA and 5'-TpG steps. The connectivity of NOE interactions between the C6-H or C8-H of a particular base and its own sugar H-2' to make intranucleotide connections and between the C6-H or C8-H and the sugar H-2'' of the nucleotide on the 5' side of the sequence to assign the residues sequentially confirmed this site of intercalation. The characteristic adenine³ C8-H/cytosine² H-2'' and thymine⁴ H-2''/guanine⁵ C8-H NOESY contacts were

(44) Boger, D. L.; Saionz, K. Unpublished studies. Tables 6 and 7 (supporting information) provide the nucleic acid and sandramycin proton chemical shift assignments in the d(GCATGC)₂–sandramycin complex along with their comparisons with free agent, free DNA, and the analogous luzopeptin A complexes taken from refs 29 and 30. Full refinements of this structure are in progress and will be disclosed in full detail in due time.

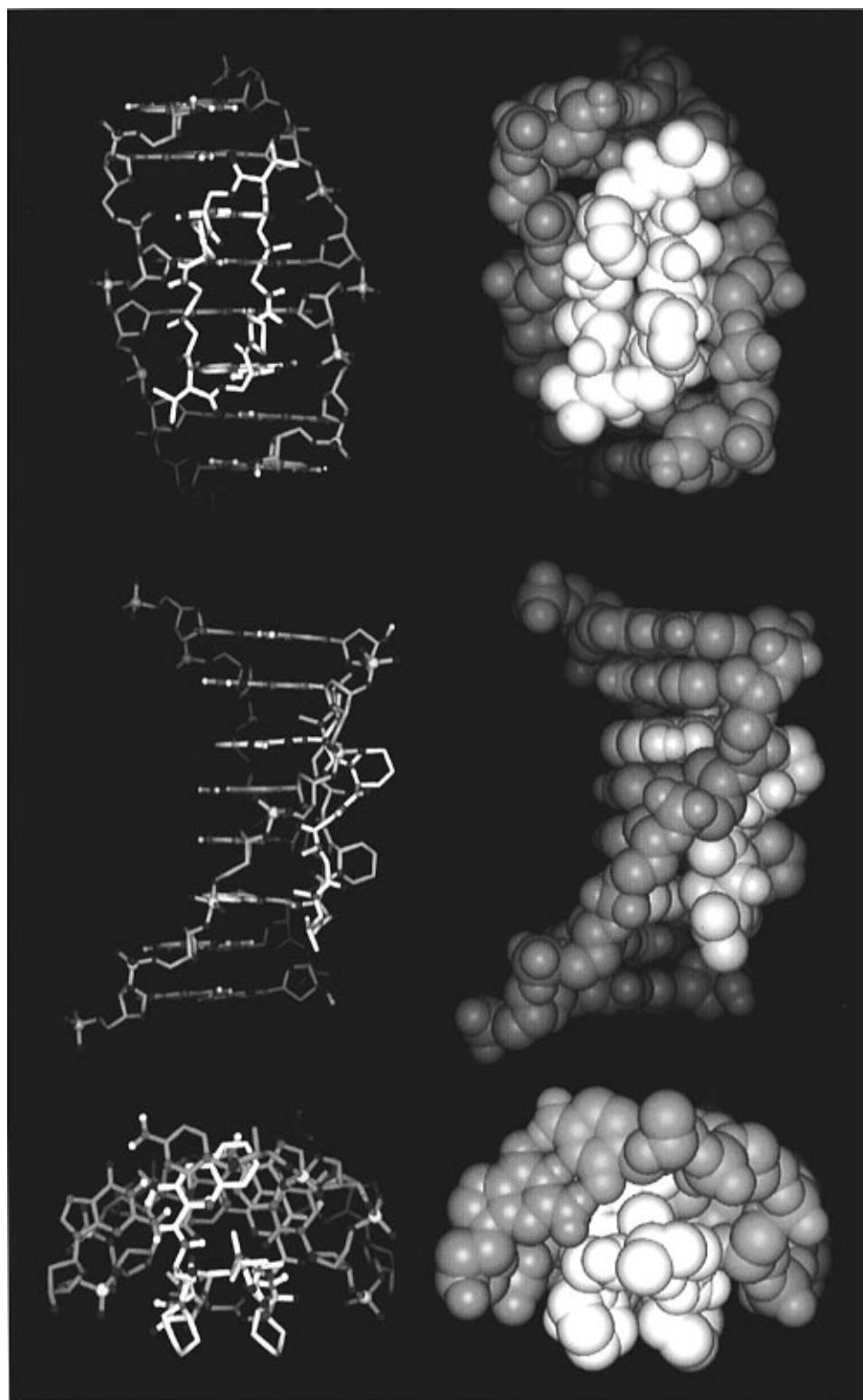


Figure 5. Three views of the 5'-d(GCATGC)₂-sandramycin complex illustrating the symmetrical minor groove binding of the cyclic decadepsipeptide (top and bottom) and the bisintercalation sandwiching the central two A-T base pairs (middle).

interrupted and absent in the complex while the intense NOE linking thymine⁴ C5-CH₃ and adenine³ C8-H was unperturbed. Similarly, the guanine¹ H-2''/cytosine² C6-H, adenine³ H-2''/thymine⁴ C6-H, and guanine⁵ H-2''/cytosine⁶ C6-H NOE connectivity were unperturbed. In addition, the connectivities between the base protons and the sugar H-1' could be used to trace the chain by monitoring the NOEs between the base C8-H or C6-H protons and their own and the 5' flanking sugar H-1' protons. This also clearly established bisintercalation with chromophore insertion between the 5'CpA and 5'-TpG sites. Notably absent in the complex were the adenine³ C8-H/cytosine²

H-1' as well as the guanine⁵ C8-H/thymine⁴ H-1' NOEs while the interresidue cytosine² C6-H/guanine¹ H-1' thymine⁴ C6-H/adenine³ H-1', cytosine⁶ C6-H/guanine⁵ H-1' NOEs were unperturbed in the complex. Additional quinoline-nucleic acid base NOE contacts and a rich array of cyclic decadepsipeptide-nucleic acid NOE contacts clearly indicate the minor groove binding in addition to the intercalation orientation analogous to the complexes of luzopeptin which have been described in detail.^{29,30} The cyclic decadepsipeptide is positioned in the minor groove of the duplex and, like luzopeptin, most likely adopts a conformation in which the pip-gly and gly-sar amides

Table 5. In Vitro Cytotoxic Activity^a

agent	IC ₅₀ , nM				
	Molt-4	L1210	786-0	Ovar-3	B16
luzopeptin A	0.8	0.02	0.2	6	0.07
sandramycin	0.8	0.02	4	2	0.4
27	4	20-2	120	60	8
32	400	500	nt	nt	nt
25	>10 ⁵	>10 ⁵	80 000	80 000	nt
24	>10 ⁵	>10 ⁵	80 000	80 000	nt
21	>10 ⁵	>10 ⁵	50 000	60 000	nt
15	5000	>10 ⁵	80 000	50 000	nt

^a Molt-4 (human T-cell leukemia), L1210 (mouse leukemia), 786-0 (human perirenal cell carcinoma), Ovar-3 (human ovarian carcinoma), B16 (melanoma).

are *cis* to accommodate the bisintercalation sandwiching the central A-T base pairs.³⁰ Complementary intermolecular hydrophobic contacts between the agent and DNA extend over much of the interacting surface. Although our studies are preliminary and not yet refined,⁴⁴ they established that sandramycin and luzopeptin interact with 5'-d(GCATGC)₂ in an analogous fashion. Illustrated in Figure 5 is a model of the 5'-(GCATGC)₂ complex with sandramycin constructed on the basis of the structure of the luzopeptin complex^{8,30} established by Patel and Zhang which highlights the minor groove binding and bisintercalation spanning the central two A-T base pairs.

In Vitro Cytotoxic Activity. Table 5 summarizes the comparison in vitro cytotoxic activities of luzopeptin A, the most potent of the naturally occurring luzopeptins, and sandramycin alongside that of the key partial structures including its bis benzyl ether **27**, the cyclic decadepsipeptide **32** possessing a single chromophore, the cyclic decadepsipeptides **24** and **25** lacking both chromophores, the linear decadepsipeptide **21**, and the linear pentadepsipeptide **15**. Consistent throughout the five assays, luzopeptin A and sandramycin exhibit comparable and exceptionally potent cytotoxic activity (6–0.02 nM). The bis benzyl ether **27** was generally 20–100× less potent than **1** and the results represent a consistent general observation that alkylation of the quinoline C3 phenol diminishes biological potency.⁴⁵ However, the impact of the introduction of this bulky benzyl ether is smaller than anticipated but consistent with the subsequent finding that the removal of the phenol altogether results in little change in the cytotoxic activity.⁴⁵ Consequently, the diminished properties of **27** most likely may be attributed to the introduction of unfavorable steric interactions which diminish the agents intercalation capabilities rather than lost H-bonding capabilities. The agent **32** possessing a single chromophore proved to be approximately 500–1000× less potent than **1** and the cyclic decadepsipeptides **24** and **25** lacking both chromophores were inactive and ≥10⁵× less potent than **1**. Similarly, the linear decadepsipeptide **21** and pentadepsipeptide **15** were inactive.

Conclusions. A concise and efficient total synthesis of sandramycin amendable to the preparation of analogs was reported which served to confirm the structure and stereochemistry of the natural product and provided key partial structures. Preliminary studies of the DNA binding properties revealed that sandramycin possesses a DNA binding constant slightly greater than that of luzopeptin A, binds to DNA with a higher selectivity than luzopeptin A (saturated binding at a 1:6.7 vs 1:4.5 agent/base pair ratio), and induces the unwinding of negatively supercoiled ΦX174 DNA and its rewinding or positive supercoiling characteristic of bisintercalation at lower agent concentrations than luzopeptin A. Both sandramycin and luzopeptin bind at least 10× more tightly than echinomycin⁷ and exhibit extraordinarily slow off rates.⁸ Sandramycin and luzopeptin A

were substantially more effective than **32** lacking one chromophore and much more effective than **25** lacking both chromophores. The largest share of the binding affinity is derived from the cyclic decadepsipeptide ($\Delta G^\circ = -6.0$ kcal/mol) and the addition of each chromophore was found to incrementally increase the affinity by approximately 3.2 and 1.0 kcal/mol, respectively. This is consistent with its representation as cyclic decadepsipeptide minor groove binding agent incrementally stabilized by mono and bisintercalation. Studies of the unwinding of supercoiled DNA and its subsequent rewinding confirmed bisintercalation binding. DNase I footprinting studies revealed that sandramycin and luzopeptin A behave similarly and appear to bind best to regions containing alternating A and T residues. Binding at other and perhaps all sites is observed at modest agent concentrations although a perceptible preference for 5'-CAT was noted. Preliminary studies of the 1:1 complex of sandramycin with 5'-d(GCATGC)₂ revealed that it forms a complex analogous to that observed with luzopeptin A. The agent sandwiches the central two Watson-Crick A-T base pairs and adopts a compact conformation in which the interchromophore distance is 10.1 Å (vs 17–19 Å). This suggests that the relatively low contribution to the binding affinity that is attributable to the second intercalation is due to an accompanying destabilizing conformational change in the cyclic decadepsipeptide that offsets much of the gains derived from the second intercalation. The cyclic decadepsipeptide is positioned in the minor groove and adopts a compact conformation that permits a rich array of complementary hydrophobic contacts extending over much of the interacting surface.

Experimental Section

Boc-Gly-Sar-OMe (2). A solution of Boc-Gly-OH (2.70 g, 15.4 mmol) and the HCl salt of H₂N-Sar-OMe (2.15 g, 15.4 mmol) in CH₂Cl₂ (50 mL) was treated sequentially with Et₃N (2.2 mL, 15.8 mmol), DCC (3.20 g, 15.5 mmol), and DMAP (306 mg, 2.5 mmol), and the reaction mixture was stirred at 25 °C for 20 h. A white precipitate formed in the first 10 min and was removed by filtration at the end of the reaction. The filtrate was concentrated in vacuo. Flash chromatography (SiO₂, 5 × 16 cm, 40% EtOAc-hexane eluent) afforded **2** (3.21 g, 4.01 g, theoretical, 80%) as a colorless oil which solidified on standing: mp 72–73 °C (EtOAc-hexane, colorless cubes); *R*_f = 0.32 (50% EtOAc-hexane); ¹H NMR (CDCl₃, 400 MHz) (4:1 mixture of two conformers, for the major conformer) δ 5.44 (s, 1H), 4.14 (s, 2H), 4.02 (d, 2H, *J* = 4.3 Hz), 3.73 (s, 3H), 3.02 (s, 3H), 1.43 (s, 9H); ¹³C NMR (CDCl₃, 100 MHz) for major conformer: δ 169.3, 168.7, 155.7, 79.6, 52.2, 49.4, 42.2, 35.2, 28.3; IR (KBr) *ν*_{max} 3419, 2978, 2934, 1754, 1715, 1667, 1488, 1424, 1367, 1249, 1208, 1175, 1120, 1051, 952, 871, 764, 712 cm⁻¹; FABHRMS (NBA-NaI) *m/z* 283.1259 (M + Na⁺, C₁₁H₂₀N₂O₅; requires 283.1270).

Anal. Calcd for C₁₁H₂₀N₂O₅: C, 50.75; H, 7.74; N, 10.76. Found: C, 50.96; H, 7.62; N, 10.63.

Boc-Gly-Sar-OH (3). Lithium hydroxide monohydrate (598 mg, 14.3 mmol) was added to a solution of **2** (1.22 g, 4.7 mmol) in 20 mL of THF-CH₃OH-H₂O (3:1:1) at 25 °C and the resulting reaction mixture was stirred for 3 h. The reaction mixture was poured onto 3 M aqueous HCl (10 mL) and extracted with EtOAc (3 × 20 mL). The combined organic phases were dried (Na₂SO₄), filtered, and concentrated in vacuo to give **3**¹⁴ (1.16 g, 1.16 g theoretical, 100%) as a colorless oil. This acid was identical to authentic material¹⁴ and was used directly in the next step without further purification: ¹H NMR (CDCl₃, 400 MHz)¹⁴ δ 5.76 and 5.66 (two br s, 1H), 4.11, 4.00, and 3.91 (three s, 4H), 2.99 and 2.95 (two s, 3H), 1.38 (s, 9H); IR (neat) *ν*_{max} 3348, 2979, 2937, 1717, 1654, 1691, 1409, 1368, 1287, 1252, 1167, 1053, 1030, 954, 866, 782, 736 cm⁻¹.

Boc-Gly-Sar-NMe-Val-OMe (6). A solution of **3**¹⁴ (1.81 g, 7.4 mmol) and the HCl salt of **5**¹⁵ (1.34 g, 7.4 mmol) in CH₂Cl₂ (40 mL) was treated sequentially with Et₃N (1.1 mL, 7.9 mmol, 1.05 equiv), DCC (1.52 g, 7.4 mmol), and DMAP (93 mg, 0.76 mmol, 0.1 equiv), and the reaction mixture was stirred at 25 °C for 24 h. A white

(45) Boger, D. L.; Chen, J.-H. Unpublished studies.

precipitate formed in the first 15 min and was removed by filtration at the end of the reaction. The filtrate was concentrated in vacuo. Flash chromatography (SiO₂, 4 × 16 cm, 50% EtOAc–hexane eluent) afforded **6** (2.04 g, 2.75 g theoretical, 74%) as a colorless oil: $R_f = 0.22$ (66% EtOAc–hexane); $[\alpha]_D^{23} -62$ (c 2.6, CHCl₃); ¹H NMR (CDCl₃, 400 MHz) mixture of multiple conformers, δ 5.42 (br s, 1H), 4.82 (d, 0.6H, $J = 10.6$ Hz), 4.37–4.00 (m, 4H), 3.79 (d, 0.4 H, $J = 10.9$ Hz), 3.72–3.67 (three s, 3H), 3.00–2.84 (six s, 6H), 2.30–2.10 (m, 1H), 1.41 and 1.40 (two s, 9H), 0.94 and 0.84 (two d, 6H, $J = 6.6$ Hz); IR (neat) ν_{\max} 3421, 2969, 2934, 1740, 1712, 1655, 1485, 1404, 1366, 1291, 1251, 1204, 1170, 1051, 1617, 952, 870, 835, 781 cm⁻¹; CIHRMS (isobutane) m/z 374.2303 (C₁₇H₃₁N₃O₆ requires 374.2291).

Boc-Gly-Sar-NMe-Val-OBn (20). A solution of **3** (4.65 g, 18.9 mmol) and the HCl salt of **19**²⁵ (4.87 g, 18.9 mmol) in CH₂Cl₂ (100 mL) was treated sequentially with Et₃N (3 mL, 21.5 mmol, 1.1 equiv), DMAP (1.15 g, 9.4 mmol, 0.5 equiv), and DCC (3.90 g, 18.9 mmol), and the reaction mixture was stirred at 25 °C for 24 h. A white precipitate formed during the reaction and was removed by filtration. The filtrate was concentrated in vacuo. Flash chromatography (SiO₂, 6 × 20 cm, 50% EtOAc–hexane eluent) afforded **20** (7.21 g, 8.49 g theoretical, 85%) as a white crystalline solid which was further recrystallized from EtOAc–hexane; mp 97–99 °C; $R_f = 0.21$ (50% EtOAc–hexane); $[\alpha]_D^{23} -63$ (c 0.8, CHCl₃); ¹H NMR (CDCl₃, 400 MHz) δ 7.32 (m, 5H), 5.43 (br s, 1H), 5.16, 5.15, 5.13 (3s, 2H), 4.88 (d, 0.7H, $J = 10.4$ Hz), 4.41, 4.30, 4.11, 4.05 (4d, 2H, $J = 16$ Hz), 4.00 (dd, 1.3H, $J = 1.7, 4.3$ Hz), 3.96 (d, 0.7H, $J = 4.3$ Hz), 3.84 (d, 0.3H, $J = 10.4$ Hz), 2.98, 2.93, 2.89 (3s, 3H), 2.90, 2.85, 2.83 (3s, 3H), 2.33–2.15 (m, 1H), 1.43, 1.42, 1.41 (3s, 9H), 0.95, 0.91, 0.84 (3d, 6H, $J = 6.6$ Hz); ¹³C NMR for the major rotamer (CDCl₃, 100 MHz) δ 170.6, 169.1, 168.3, 155.7, 135.5, 128.5, 128.3, 128.2, 79.5, 66.5, 61.9, 49.6, 42.2, 35.3, 30.6, 28.3, 27.5, 19.6, 19.0; IR (KBr) ν_{\max} 3337, 2973, 1736, 1706, 1664, 1534, 1473, 1394, 1296, 1249, 1186, 1052, 955, 742, 703 cm⁻¹.

Anal. Calcd for C₂₃H₃₅N₃O₆: C, 61.45; H, 7.85; N, 9.35. Found: C, 61.44; H, 7.81; N, 9.23.

Boc-Gly-Sar-NMe-Val-OH (7). From **6**. Lithium hydroxide mono-hydrate (249 mg, 5.9 mmol) was added to a solution of **6** (740 mg, 1.98 mmol) in 15 mL of THF–CH₃OH–H₂O (3:1:1) at 25 °C and the resulting reaction mixture was stirred for 3 h. The reaction mixture was poured onto 3 M aqueous HCl (8 mL) and extracted with EtOAc (3 × 20 mL). The combined organic phases were dried (Na₂SO₄), filtered, and concentrated in vacuo to give **7** (638 mg, 712 mg theoretical, 90%) as a white solid which was employed directly in the next reaction without further purification: white foam, mp 57–60 °C; ¹H NMR (CDCl₃, 400 MHz) δ 5.67 and 5.58 (two s, 1H), 4.63 (d, 1H, $J = 10.4$ Hz), CH, 4.10–3.82 (m, 4H), 3.05, 3.04, 3.01, and 2.88 (four s, 6H), 2.30–2.20 (m, 1H), 1.43 and 1.41 (two s, 9H), 1.04 and 0.88 (two d, 6H, $J = 6.7$ Hz); IR (KBr) ν_{\max} 3421, 2974, 1706, 1656, 1495, 1419, 1367, 1292, 1250, 1171, 1053, 953, 870, 837, 670 cm⁻¹.

From 20. A solution of **20** (2.62 g, 5.85 mmol) in 40 mL of CH₃OH was treated with 10% Pd–C (300 mg) and the resulting black suspension was stirred at 25 °C under H₂ (1 atm) for 16 h. The catalyst was removed by filtration through Celite, and the filtrate was concentrated in vacuo to give **7** (2.14 g, 2.10 g theoretical, 100%) as a white foam: $[\alpha]_D^{23} -63.3$ (c 1.1, CHCl₃); identical in all respects to the material above.

Benzyl L-Pipecolate (11). **Method A.** A solution of **9**¹⁶ (2.96 g, 12.9 mmol) in CH₂Cl₂ (60 mL) was treated sequentially with saturated aqueous NaHCO₃ (40 mL), Bu₄NI (4.76 g, 12.9 mmol, 1.0 equiv) and benzyl bromide (3.31 g, 19.4 mmol, 1.5 equiv). The resulting mixture was stirred at 25 °C under N₂ for 24 h. The reaction mixture was extracted with CH₂Cl₂ (3 × 100 mL). The combined organic layers were dried (Na₂SO₄), filtered, and concentrated in vacuo. Chromatography (SiO₂, 5 × 18 cm, 1:15 EtOAc–hexane eluent) afforded **10** (3.71 g, 4.12 g theoretical, 90%) as a white solid: mp 51–53 °C; $[\alpha]_D^{23} -48$ (c 3.4, CHCl₃); $R_f = 0.49$ (10% EtOAc–hexane); ¹H NMR revealed a 1:1 mixture of two conformers, ¹H NMR (CDCl₃, 400 MHz) δ 7.32 (m, 5H), 5.21 (s, 2H), 4.94 (br s, 0.5H), 4.74 (br s, 0.5H), 4.01 (d, 0.5H, $J = 12.0$ Hz), 3.90 (d, 0.5H, $J = 12.0$ Hz), 2.91 (m, 1H), 2.22 (m, 1H), 1.70–1.10 (m, 5H), 1.44 (s, 4.5H), 1.36 (s, 4.5H); ¹³C NMR (CDCl₃, 100 MHz) δ 172.0, 171.8, 156.0, 155.4, 135.8, 128.5, 128.2, 128.1, 127.9, 79.9, 66.6, 54.9, 53.8, 42.1, 41.1, 28.3, 28.2, 26.7, 24.8, 24.5, 20.8, 20.6; IR (KBr) ν_{\max} 2941, 2861, 1734, 1700, 1454, 1364,

1340, 1246, 1154, 1091, 1045, 1002, 930, 873, 783, 752, 697 cm⁻¹; FABHRMS (NBA–NaI) m/z 342.1672 (M + Na⁺, C₁₈H₂₅NO₄ requires 342.1681).

Method B. A solution of *N*-BOC-Pip-OH¹⁶ (**9**, 1.28 g, 5.6 mmol) and benzyl alcohol (1.05 g, 9.7 mmol, 1.7 equiv) in CH₂Cl₂ (20 mL) was cooled to –30 °C and sequentially treated with DMAP (68.3 mg, 0.56 mmol, 0.1 equiv) and DCC (1.16 g, 5.6 mmol, 1.0 equiv). The resulting mixture was stirred at –30 °C under Ar for 2.0 h. The white precipitate of DCU was removed by filtration, and the filtrate was concentrated in vacuo. Chromatography (SiO₂, 4 × 16 cm, 1:15 EtOAc–hexane eluent) afforded **10** (1.74 g, 1.79 g theoretical, 97%) as a white solid: mp 51–53 °C; $[\alpha]_D^{23} -46$ (c 2.7, CHCl₃); identical in all respects to the material above.

A sample of **10** (6.73 g, 21.1 mmol) in a 100 mL round-bottom flask was treated with 3 M HCl–EtOAc (40 mL, 120 mmol, 5.7 equiv). The resulting mixture was stirred at 25 °C for 30 min. The volatiles were removed in vacuo. The residual HCl was further removed by adding Et₂O (40 mL) to the hydrochloride salt of **11** followed by its removal in vacuo. After repeating this procedure three times, 5.38 g of the hydrochloride salt of **11** (5.39 g theoretical, 100%) was obtained. The hydrochloride salt of **11** was neutralized with saturated aqueous NaHCO₃ (50 mL) and extracted with EtOAc (3 × 100 mL). The combined organic layers was dried (Na₂SO₄), filtered, and concentrated in vacuo to give **11** (4.62 g, 4.61 g theoretical, 100%) as white crystalline plates: mp 146–148 °C; $[\alpha]_D^{23} -23.3$ (c 0.7, CHCl₃); ¹H NMR (CDCl₃, 400 MHz) δ 7.33 (m, 5H), 5.24 (d, 1H, $J = 12.2$ Hz), 5.18 (d, 1H, $J = 12.2$ Hz), 3.97 (dd, 1H, $J = 4.0, 10.0$ Hz), 3.56 (ddd, 1H, $J = 4.2, 4.5, 12.9$ Hz), 3.06 (ddd, 1H, $J = 3.4, 10.1, 12.9$ Hz), 2.27–2.21 (m, 1H), 2.15–2.06 (m, 1H), 2.01–1.97 (m, 1H), 1.84–1.73 (m, 2H), 1.60–1.52 (m, 1H); ¹³C NMR (CDCl₃, 100 MHz) δ 168.2, 134.6, 128.7, 128.6, 128.4, 68.0, 56.3, 43.7, 25.6, 21.6, 21.5; IR (KBr) ν_{\max} 3347, 2934, 2853, 1737, 1453, 1257, 1179, 1126, 1052, 749, 698 cm⁻¹; FABHRMS (NBA–NaI) m/z 220.1345 (M + H⁺, C₁₃H₁₇NO₂ requires 220.1338).

***N*-SES-D-Ser-OBn (12).** Solution of D-serine benzyl ester (4.38 g, 22.4 mmol) and Et₃N (3.2 mL, 23.0 mmol) in 90 mL of degassed anhydrous DMF at –30 °C was treated slowly with trimethylethane-sulfonyl chloride (4.50 g, 22.4 mmol). The reaction mixture was stirred at –30 °C under Ar for 9 h and poured onto 100 mL of H₂O and extracted with EtOAc (3 × 150 mL). The combined organic layers were washed with saturated aqueous NaCl (150 mL), dried (Na₂SO₄), filtered, and concentrated in vacuo. Flash chromatography (SiO₂, 5 × 20 cm, 20–40% EtOAc–hexane gradient) to afford **12** (6.84 g, 8.05 g theoretical, 85%) as a colorless oil: $[\alpha]_D^{23} -2.2$ (c 1.5, CHCl₃); $R_f = 0.48$ (SiO₂, 50% EtOAc–hexane); ¹H NMR (CDCl₃, 400 MHz) δ 7.35 (m, 5H), 5.41 (d, 1H, $J = 8.5$ Hz), 5.22 (s, 2H), 4.24 (dt, 1H, $J = 11.2, 3.4$ Hz), 4.00 (dd, 1H, $J = 11.2, 3.8$ Hz), 3.93 (dd, 1H, $J = 11.2, 3.4$ Hz), 3.00–2.90 (m, 2H), 1.10–0.98 (m, 2H), 0.01 (s, 9H); ¹³C NMR (CDCl₃, 50 MHz) δ 171.0, 135.5, 129.2, 129.1, 128.8, 68.1, 64.4, 58.4, 50.4, 10.5, –1.9; IR (neat) ν_{\max} 3504, 3288, 2954, 1742, 1498, 1330, 1252, 1174, 1130, 1070, 966, 894, 862, 842, 738, 698 cm⁻¹; FABHRMS (NBA) m/z 359.1220 (C₁₅H₂₅NO₅SiS requires 359.1223).

***N*-SES-D-Ser-OH (13).** A solution of **12** (1.05 g, 2.91 mmol) in CH₃OH (20 mL) was treated with 10% Pd–C (100 mg). The resulting black suspension solution was stirred under H₂ (1 atm) at 25 °C for 12 h. The catalyst was removed by filtration through Celite, and the filtrate was concentrated in vacuo to give **13** (785 mg, 784 mg theoretical, 100%) as a white solid: mp 61–63 °C; $[\alpha]_D^{23} -2.1$ (c 2.2, CHCl₃); ¹H NMR (CDCl₃, 400 MHz) δ 6.12 (d, 1H, $J = 8.7$ Hz), 5.42 (br s, 2H), 4.20 (d, 1H, $J = 8.7$ Hz), 4.11 (d, 1H, $J = 10.2$ Hz), 3.92 (d, 1H, $J = 10.2$ Hz), 3.05–2.96 (m, 2H), 1.10–0.98 (m, 2H), 0.04 (s, 9H); ¹³C NMR (CDCl₃, 100 MHz) δ 173.3, 64.2, 57.7, 50.2, 10.2; IR (KBr) ν_{\max} 3416, 3313, 2956, 1740, 1321, 1252, 1177, 1120, 1023, 843, 759, 741, 700 cm⁻¹; FABHRMS (NBA–NaI) m/z 292.0663 (M + Na⁺, C₈H₁₉NO₅SiS requires 292.0651).

Anal. Calcd for C₈H₁₉NO₅SiS: C, 35.67; H, 7.11; N, 5.20; S, 11.90. Found: C, 35.93; H, 6.96; N, 5.39; S, 12.24.

***N*-SES-D-Ser-Pip-OBn (14).** A solution of **11**¹⁶ (1.27 g, 5.77 mmol, 1.3 equiv) and **13** (1.23 g, 4.58 mmol) in CH₂Cl₂ (20 mL) was cooled to 0 °C and sequentially treated with Et₃N (1.90 mL, 13.6 mmol, 3.0 equiv) and bis(2-oxo-3-oxazolidinyl)phosphinic chloride (BOP–Cl, 1.62 g, 6.36 mmol, 1.40 equiv), and the resulting reaction mixture was stirred

at 0 °C for 10 h. The reaction mixture was diluted with CH₂Cl₂ (50 mL) and washed sequentially with 10% aqueous HCl (30 mL), H₂O (30 mL), saturated aqueous NaHCO₃ (30 mL), and saturated aqueous NaCl (30 mL). The organic layer was dried (Na₂SO₄), filtered, and concentrated in vacuo. Flash chromatography (SiO₂, 4 × 16 cm, 40% EtOAc–hexane eluent) afforded **14** (1.83 g, 2.15 g theoretical, 85%) as a white crystalline solid: mp 105–106 °C; *R*_f = 0.35 (50% EtOAc–hexane); [α]_D²³ –72 (*c* 1.1, CH₂Cl₂); ¹H NMR (CDCl₃, 400 MHz) δ 7.39–7.31 (m, 5H), 5.55 (d, 1H, *J* = 8.7 Hz), 5.30 (d, 1H, *J* = 5.2 Hz), 5.20 (d, 1H, *J* = 12.3 Hz), 5.09 (d, 1H, *J* = 12.3 Hz), 4.50 (m, 1H), 3.79–3.68 (m, 2H), 3.30 (dt, 1H, *J* = 3.0, 13.1 Hz), 2.95–2.87 (m, 2H), 2.66 (m, 1H), 2.31 (d, 1H, *J* = 14.2 Hz), 1.76–1.18 (m, 6H), 1.06–0.98 (m, 2H), 0.03 (s, 9H); ¹³C NMR (CDCl₃, 100 MHz) δ 170.1, 169.9, 135.3, 128.6, 128.4, 128.0, 67.1, 64.3, 55.4, 53.0, 49.5, 43.6, 26.3, 25.0, 20.7, 10.1, –2.1; IR (KBr) *ν*_{max} 3466, 3270, 2950, 2860, 1738, 1643, 1418, 1322, 1250, 1162, 1143, 1017, 843, 738, 698 cm⁻¹; FABHRMS (NBA) *m/z* 471.1985 (M⁺ + H, C₂₁H₃₄N₂O₆SiS requires 471.1985).

Anal. Calcd for C₂₁H₃₄N₂O₆SiS: C, 53.59; H, 7.28; N, 5.95; S, 6.81. Found: C, 53.68; H, 7.19; N, 6.11; S, 6.83.

N-SES-D-Ser[Gly-Sar-NMe-Val]-Pip-OBn (15). A solution of **14** (2.76 g, 5.85 mmol) and **7** (2.10 g, 5.86 mmol) in CH₂Cl₂ (40 mL) was cooled to 0 °C and sequentially treated with DMAP (0.71 g, 5.86 mmol, 1.0 equiv) and DCC (1.21 g, 5.86 mmol, 1.0 equiv), and the resulting reaction mixture was stirred at 0 °C for 24 h. The white precipitate that formed was removed by filtration, and the filtrate was concentrated in vacuo. Flash chromatography (SiO₂, 4 × 16 cm, 50% EtOAc–hexane eluent) afforded **15** which was separated into two isomers. The major isomer constitutes the desired product **15** (3.75 g, 79%, typically 79–89%) and the minor isomer constitutes the Val α-CH epimerized product (300 mg, 6%).

For the Major Diastereomer 15: White foam; mp 68–72 °C; *R*_f = 0.44 (67% EtOAc–hexane); [α]_D²³ –110 (*c* 2.0, CHCl₃); ¹H NMR (CDCl₃, 400 MHz) δ 7.67 (d, 0.4 H, *J* = 9.6 Hz), 7.34–7.27 (m, 5H), 5.69–5.49 (m, 1.6H), 5.29 and 5.22 (two d, 1H, *J* = 6.7 Hz), 5.21–4.90 (m, 3H), 4.79 (d, 1H, *J* = 10.7 Hz), 4.75–4.35 (m, 2H), 4.15–3.55 (m, 4H), 3.35–3.20 (m, 1H), 3.05–2.70 (four s and a set of multiplets, 8H), 2.32–2.15 (m, 2H), 1.75–1.15 (m, 15H), 1.05–0.82 (m and three d, 8H, *J* = 6.4 Hz), –0.05 to –0.08 (several s, 9H); IR (KBr) *ν*_{max} 3223, 2956, 1740, 1708, 1658, 1485, 1416, 1325, 1250, 1168, 1018, 841 cm⁻¹; FABHRMS (NBA) *m/z* 812.9362 (M⁺ + H, C₃₇H₆₁N₅O₁₁SiS requires 812.9362).

Anal. Calcd for C₃₇H₆₁N₅O₁₁SiS: C, 54.72; H, 7.57; N, 8.62; S, 3.95. Found: C, 55.00; H, 7.65; N, 8.70; S, 4.13.

For the Minor Isomer: White foam; mp 72–76 °C *R*_f = 0.35 (67% EtOAc–hexane); [α]_D²³ –36 (*c* 0.15, CHCl₃); ¹H NMR (CDCl₃, 400 MHz) δ 7.35–7.25 (m, 5H), 5.86 (d, 1H, *J* = 9.2 Hz), 5.68–5.61 (m, 1H), 5.28–5.00 (m, 3H), 4.82 (d, 1H, *J* = 10.8 Hz), 4.67 (m, 1H), 4.50–3.80 (m, 6H), 3.31 (m, 1H), 3.04–2.79 (two s and a set of multiplets, 8H), 2.32–2.15 (m, 2H), 1.80–1.35 (m, 15H), 1.05–0.83 (two d and m, 8H, *J* = 6.7 Hz), 0.01 (s, 9H); IR (KBr) *ν*_{max} 3421, 3237, 2962, 1741, 1657, 1325, 1250, 1167, 1051, 1017, 972, 842, 742, 700 cm⁻¹; FABHRMS (NBA–CsI) *m/z* 944.2922 (M + Cs⁺, C₃₇H₆₁N₅O₁₁SiS requires 944.2912).

N-SES-D-Ser[N-SES-D-Ser[Gly-Sar-NMe-Val]-Pip-Gly-Sar-NMe-Val]-Pip-OBn (21). A solution of **15** (1.62 g, 2.0 mmol) in CH₃OH (30 mL) was treated with 10% Pd–C (160 mg) and the resulting black suspension was stirred at 25 °C under H₂ (1 atm) for 12 h. The catalyst was removed by filtration through Celite and the filtrate was concentrated in vacuo to give the crude acid **17** (1.45 g, 1.45 g theoretical, 100%) which was used directly in the next reaction without further purification.

Another 1.62 g sample of **15** (2.0 mmol) was treated with 10 mL of 3 M HCl–EtOAc and the mixture was stirred at 25 °C for 30 min. The volatiles were removed in vacuo. The residual HCl was removed by adding Et₂O (15 mL) to the hydrochloride salt **16** followed by its removal in vacuo. After repeating this procedure three times, 1.50 g of **16** (1.49 g theoretical, 100%) was obtained and used directly in the following reaction without further purification.

A solution of **17** (1.45 g, 2.0 mmol) and the hydrochloride salt **16** (1.50 g, 2.0 mmol) in DMF (10 mL) was treated sequentially with NaHCO₃ (675 mg, 8.0 mmol), HOBT (271 mg, 2.0 mmol), and EDCl (385 mg, 2.0 mmol), and the reaction mixture was stirred at 0 °C (2 h)

and 25 °C (24 h). The reaction mixture was poured onto H₂O (20 mL) and extracted with EtOAc (3 × 40 mL). The combined organic phase was washed with saturated aqueous NaCl (20 mL), dried (Na₂SO₄), filtered and concentrated in vacuo. Flash chromatography (SiO₂, 2 × 16 cm, 80–100% EtOAc–CH₂Cl₂ gradient elution) afforded **21** (2.28 g, 2.84 g theoretical, 80%) as a glassy solid: *R*_f = 0.6 (5% CH₃CN–EtOAc); [α]_D²³ –124 (*c* 0.9, CHCl₃); ¹H NMR (CDCl₃, 400 MHz) δ 7.36–7.26 (m, 5H), 5.70–5.50 (m, 2H), 5.30–5.05 (m, 4H), 4.80–3.60 (m, 16H), 3.40–3.20 (m, 2H), 3.10–2.70 (m, 16H), 2.35–2.10 (m, 4H), 1.85–1.20 (m, 21H), 1.05–0.80 (two d and m, 16H, *J* = 6.2 Hz and 6.5 Hz), 0.01 to –0.08 (m, 18H); IR (KBr) *ν*_{max} 3240, 2954, 1740, 1655, 1482, 1456, 1415, 1318, 1287, 1250, 1169, 1021, 841, 739 cm⁻¹; FABHRMS (NBA–NaI) *m/z* 1437.6599 (M + Na⁺, C₆₂H₁₀₆N₁₀O₁₉Si₂S₂ requires 1437.6531).

(N-SES-D-Ser-Pip-Gly-Sar-NMe-Val)₂ (Serine Hydroxyl) Dilactone (24). A solution of **21** (1.69 g, 1.14 mmol) in CH₃OH (20 mL) was treated with 10% Pd–C (200 mg), and the black suspension was stirred at 25 °C under an atmosphere of H₂ (1 atm) for 16 h. The catalyst was removed by filtration through Celite, and the filtrate was concentrated in vacuo to give crude **22** (1.47 g, 1.51 g theoretical, 97%). Crude **19** was treated with 3 M HCl–EtOAc (10 mL), and the mixture was stirred at 25 °C for 30 min. The volatiles were removed in vacuo, and the excess HCl was removed by suspending the hydrochloride salt in Et₂O (30 mL) followed by its removal in vacuo. After this procedure was repeated three times, 1.41 g (1.40 g theoretical, 100%) of the hydrochloride salt **23** was obtained and used in the next step without further purification.

A solution of the hydrochloride salt **23** (1.41 g, 1.11 mmol) in degassed DMF (370 mL) cooled to 0 °C and sequentially treated with NaHCO₃ (933 mg, 11.1 mmol, 10 equiv) and diphenyl phosphorazidate (DPPA, 0.86 mL, 4.45 mmol, 4.0 equiv), and the reaction mixture was stirred at 0 °C for 72 h. The mixture was concentrated in vacuo, and the residue was diluted with EtOAc (100 mL). The organic phase was washed with 10% aqueous HCl (50 mL), H₂O (50 mL), saturated aqueous NaHCO₃ (50 mL) and saturated aqueous NaCl (50 mL), dried (Na₂SO₄), filtered, and concentrated in vacuo. Flash chromatography (SiO₂, 2 × 16 cm, 10% CH₃CN–EtOAc eluent) afforded **24** (1.21 g, 1.36 g theoretical, 89%, typically 85–90%) as a white powder: mp 185–188 °C dec; *R*_f = 0.5 (5% CH₃CN–EtOAc); [α]_D²³ –88 (*c* 0.85, CHCl₃); ¹H NMR (CDCl₃, 400 MHz) δ 8.38 (d, 2H, *J* = 4.5 Hz, Gly-NH), 5.79 (d, 2H, *J* = 6.7 Hz, D-Ser-NH), 5.30 (d, 2H, *J* = 16.7 Hz, Sar-α-CH), 5.25 (d, 2H, *J* = 4.6 Hz, Pip-α-CH), 4.78 (d, 2H, *J* = 10.9 Hz, Val-α-CH), 4.63 (d, 4H, *J* = 8.6 Hz, D-Ser-α-CH and β-CH), 4.40 (d, 2H, *J* = 10.4 Hz, D-Ser-β-CH), 4.38 (dd, 2H, *J* = 5.6, 18.0 Hz, Gly-α-CH), 3.99 (d, 2H, *J* = 18 Hz, Gly-α-CH), 3.90 (dd, 2H, *J* = 10.8, 12.6 Hz, Pip-ε-CH), 3.55 (d, 2H, *J* = 13.4 Hz, Pip-ε-CH), 3.42 (d, 2H, *J* = 16.7 Hz, Sar-α-CH), 2.94 (s, 6H, NCH₃), 2.91 (s, 6H, NCH₃), 2.98–2.82 (m, 4H, SO₂CH₂), 2.16–2.07 (d split septet, 2H, *J* = 10.3, 6.7 Hz, Val-β-CH), 1.76–1.36 (m, 12H, Pip-(CH₂)₃), 1.04–0.94 (m, 4H, SO₂CH₂CH₂), 0.95 (d, 6H, *J* = 6.7 Hz, Val-γ-CH₃), 0.84 (d, 6H, *J* = 6.7 Hz, Val-γ-CH₃), 0.03 (s, 18H, SiMe₃); ¹³C NMR (CDCl₃, 100 MHz) δ 172.2, 169.3, 169.2, 167.7, 166.6, 65.2, 62.3, 53.7, 52.9, 49.5, 49.3, 44.0, 41.9, 35.0, 30.3, 28.4, 26.8, 24.6, 20.0, 19.3, 19.1, 10.2, –2.0; IR (KBr) *ν*_{max} 3330, 2953, 2871, 1743, 1644, 1460, 1418, 1288, 1251, 1171, 1136, 1108, 844, 738, 699 cm⁻¹; FABHRMS (NBA–CsI) *m/z* 1207.5535 (M + H⁺, C₅₀H₉₀N₁₀O₁₆S₂Si₂ requires 1207.5595).

(N-BOC-D-Ser-Pip-Gly-Sar-NMe-Val)₂ (Serine Hydroxyl) Dilactone (25). A solution of **24** (120 mg, 0.10 mmol) in THF (3 mL) was treated sequentially with (BOC)₂O (0.7 mL, 3.05 mmol, 30 equiv) and 1.0 M Bu₄NF–THF (1.0 mL, 1.0 mmol, 10 equiv), and the resulting mixture was stirred at 25 °C for 48 h. The reaction mixture was diluted with EtOAc (30 mL), washed with H₂O (20 mL) and saturated aqueous NaCl (20 mL), dried (Na₂SO₄), filtered, and concentrated in vacuo. Flash chromatography (SiO₂, 2 × 16 cm, 5% EtOH–CH₂Cl₂ eluent) afforded **25** (78 mg, 107 mg theoretical, 73%, 70–73%) as a white powder: mp 245–247 °C (EtOAc, plates); *R*_f = 0.43 (10% CH₃CN–EtOAc); [α]_D²³ –53 (*c* 0.15, CHCl₃); ¹H NMR (CDCl₃, 400 MHz) (Table 2); ¹³C NMR (CDCl₃, 100 MHz) δ 172.7, 169.31, 169.26, 167.7, 167.3, 155.1, 79.8, 63.4, 62.3, 52.6, 51.3, 49.2, 43.8, 41.8, 34.9, 30.4, 28.5, 28.4, 26.7, 24.7, 20.1, 19.5, 19.0; IR (KBr) *ν*_{max} 3422, 3333, 2964, 2937, 2862, 1742, 1713, 1647, 1491, 1458, 1368, 1290, 1250, 1167,

1014, 849, 780 cm^{-1} ; FABHRMS (NBA–CsI) m/z 1211.4985 ($\text{M} + \text{Cs}^+$, $\text{C}_{50}\text{H}_{82}\text{N}_{10}\text{O}_{16}$ requires 1211.4965).

The structure of **25** was established unambiguously in a single-crystal X-ray structure determination conducted on plates grown from EtOAc.²⁷

Sandramycin Bis-O-benzyl Ether (27). A solution **25** (48 mg, 0.044 mmol) in 3 M HCl–EtOAc (2 mL) at 25 °C was stirred for 30 min. The solvent was removed in vacuo to afford the hydrochloride salt **26** (43.3 mg, 42.3 mg theoretical, 100%) as a white powder which was used directly in next reaction.

A solution of the hydrochloride salt **26** (43.3 mg, 0.044 mmol) and **28**²⁸ (50.0 mg, 0.179 mmol, 4.0 equiv) in DMF (4 mL) was treated sequentially with NaHCO_3 (37.5 mg, 0.45 mmol, 10.2 equiv), HOBt (36.2 mg, 0.268 mmol, 6.0 equiv), and EDCI (34.3 mg, 0.178 mmol, 4.0 equiv), and the reaction mixture was stirred at 25 °C for 72 h. The reaction mixture was diluted with EtOAc (20 mL) and washed with H_2O (10 mL) and saturated aqueous NaCl (10 mL), dried (Na_2SO_4), filtered, and concentrated in vacuo. Flash chromatography (SiO_2 , 1 \times 15 cm, 5% EtOH– CH_2Cl_2 eluent) afforded **27** (56.8 mg, 62.3 mg theoretical, 91%) as a white powder: mp 270–273 °C; R_f = 0.42 (30% CH_3CN –EtOAc); $[\alpha]_D^{25}$ –107 (c 0.29, CHCl_3); $^1\text{H NMR}$ (CDCl_3 , 400 MHz) δ 9.01 (d, 2H, J = 6.3 Hz), 8.48 (d, 2H, J = 4.3 Hz), 7.92 (d, 2H, J = 7.8 Hz), 7.70 (d, 2H, J = 8.5 Hz), 7.59 (s, 2H), 7.54 (m, 8H), 7.39 (t, 4H, J = 7.5 Hz), 7.30 (t, 2H, J = 7.4 Hz), 5.46 (d, 2H, J = 4.8 Hz), 5.44 (d, 2H, J = 16.6 Hz), 5.34 (m, 6H), 4.87 (dd, 2H, J = 2.0, 11.5 Hz), 4.83 (d, 2H, J = 11 Hz), 4.58 (dd, 2H, J = 2.0, 11.5 Hz), 4.42 (dd, 2H, J = 5.7, 17.4 Hz), 4.03 (d, 2H, J = 17.4 Hz), 4.01 (m, 2H), 3.76 (d, 2H, J = 13.3 Hz), 3.47 (d, 2H, J = 16.6 Hz), 3.08 (s, 6H), 2.92 (s, 6H), 2.05 (d split septet, 2H, J = 11, 6.5 Hz), 1.80–1.40 (m, 12H), 0.95 (d, 6H, J = 6.5 Hz), 0.81 (d, 6H, J = 6.5 Hz); $^{13}\text{C NMR}$ (CDCl_3 , 100 MHz) δ 172.7, 169.2, 167.8, 167.0, 163.5, 151.7, 142.6, 141.6, 136.0, 130.2, 129.5, 128.7, 128.4, 127.9, 127.5, 126.9, 126.4, 117.2, 70.7, 62.8, 62.3, 52.5, 50.8, 49.3, 43.8, 41.9, 34.9, 30.4, 29.7, 28.7, 26.5, 24.8, 20.2, 19.4, 19.0; IR (KBr) ν_{max} 3366, 2934, 2862, 1744, 1641, 1492, 1456, 1420, 1344, 1323, 1287, 1256, 1215, 1184, 1133, 1092, 1010, 918, 841, 774, 733, 697 cm^{-1} ; FABHRMS (NBA–CsI) m/z 1533.5490 ($\text{M} + \text{Cs}^+$, $\text{C}_{74}\text{H}_{88}\text{N}_{12}\text{O}_{16}$ requires 1533.5496).

Sandramycin (1). A sample of 10% Pd–C (3 mg) was added to a solution of **27** (6.2 mg, 0.0044 mmol) in EtOAc (4 mL), and the black suspension was stirred at 25 °C under an atmosphere of H_2 (1 atm) for 12 h. The catalyst was removed by filtration through Celite, and the filtrate was concentrated in vacuo. Chromatography (SiO_2 , 0.5 \times 6 cm, EtOAc eluent) afforded **1** (4.2 mg, 5.4 mg theoretical, 78%) as a white powder identical in all respects with a sample of natural material: white powder, mp 206–209 °C, lit.¹ mp 208–212 °C; R_f = 0.4 (SiO_2 , 5% CH_3OH – CHCl_3 eluent), lit.¹ R_f = 0.4 (SiO_2 , 5% CH_3OH – CHCl_3); $[\alpha]_D^{25}$ –153 (c 0.17, CHCl_3); $^1\text{H NMR}$ (CDCl_3 , 400 MHz) δ 11.74 (s, 2H, OH), 9.56 (d, 2H, J = 5.7 Hz, Ser–NH), 8.52 (d, 2H, J = 4.4 Hz, Gly–NH), 7.81 (m, 2H, C5'–H), 7.71 (dd, 2H, J = 4.4, 5.4 Hz, C8'–H), 7.63 (s, 2H, C4'–H), 7.50 (dd, 4H, J = 4.1, 5.3 Hz, C6' and C7'–H), 5.57 (d, 2H, J = 6.4 Hz, Pip– α –CH), 5.54 (d, 2H, J = 16.6 Hz, Sar– α –CH), 5.26 (d, 2H, J = 5.0 Hz, Ser– α –CH), 4.99 (d, 2H, J = 11.7 Hz, Ser– β –CH), 4.87 (d, 2H, J = 11.0 Hz, Val– α –CH), 4.43 (d, 4H, J = 11.7 Hz, Ser– β –CH and Gly– α –CH), 4.10 (m, 2H, Pip– ϵ –CH), 4.06 (m, 2H, Gly– α –CH), 3.74 (d, J = 14.5 Hz, Pip– ϵ –CH), 3.55 (d, 2H, J = 16.6 Hz, Sar– α –CH), 3.12 (s, 6H, Val–NCH₃), 2.94 (s, 6H, Sar–NCH₃), 2.04 (d split septet, 2H, J = 11.0, 6.4 Hz, Val– β –CH), 1.85–1.50 (m, 12H, Pip–(CH₂)₃), 0.92 (d, 6H, J = 6.4 Hz, Val– γ –CH₃), 0.78 (d, J = 6.4 Hz, Val– γ –CH₃); $^{13}\text{C NMR}$ (CDCl_3 , 100 MHz) δ 172.6, 169.4, 169.2, 167.8, 167.7, 166.2, 153.8, 141.4, 134.6, 132.0, 129.4, 128.5, 127.1, 126.4, 120.3, 62.2, 61.9, 52.5, 50.6, 49.3, 43.9, 41.9, 34.9, 30.3, 28.8, 26.2, 24.9, 20.2, 19.4, 18.7; IR (KBr) ν_{max} 3487, 3329, 2932, 1744, 1662, 1637, 1518, 1468, 1418, 1333, 1285, 1191, 1135, 1016, 887, 734 cm^{-1} ; UV (CH_3OH) λ_{max} 217 (62 000), 229 (60 000), 300 (8070), 356 nm (7840); lit.¹ UV (CH_3OH) λ_{max} 217 (63 700), 229 (62 800), 356 nm (8100); FABHRMS (NBA) m/z 1221.5565 ($\text{M} + \text{H}^+$, $\text{C}_{60}\text{H}_{76}\text{N}_{12}\text{O}_{16}$ requires 1221.5581).

N^1 -SES- N^6 -Boc-(D-Ser-Pip-Gly-Sar-NMe-Val)₂ (Serine Hydroxyl) Dilactone (29). A solution of **24** (58.2 mg, 0.048 mmol) in 5 mL of THF was treated sequentially with $(\text{BOC})_2\text{O}$ (110 μL , 0.48 mmol, 10 equiv) and 1.0 M Bu_4NF in THF (192 μL , 0.192 mmol, 4 equiv). The mixture was stirred at 25 °C under N_2 for 24 h. The reaction mixture was diluted with 40 mL of EtOAc and washed with H_2O (20 mL) and saturated aqueous NaCl (20 mL). The organic layer was dried (Na_2SO_4), filtered, and concentrated in vacuo. Chromatography (SiO_2 , 2 \times 18 cm, 10% CH_3CN –EtOAc) gave **29** (18.2 mg, 55.1 mg theoretical, 33%) as a white solid along with recovered **24** (6.2 mg, 11%) and **25** (14 mg, 27%). For **29**: R_f 0.6 (30% CH_3CN –EtOAc); $[\alpha]_D^{25}$ –74 (c 0.4, CHCl_3); $^1\text{H NMR}$ (CDCl_3 , 400 MHz) δ 8.43 (d, 1H, J = 5.7 Hz), 8.42 (d, 1H, J = 6.0 Hz), 5.84 (d, 1H, J = 6.1 Hz), 5.80 (d, 1H, J = 7.2 Hz), 5.35 (d, 1H, J = 16.2 Hz), 5.31 (d, 1H, J = 16.2 Hz), 5.26 (m, 2H), 4.83 (m, 1H), 4.80 (d, 1H, J = 11.0 Hz), 4.79 (d, 1H, J = 11.0 Hz), 4.66–4.60 (m, 2H), 4.48–4.30 (m, 5H), 4.02 (d, 1H, J = 17.3 Hz), 4.00 (d, 1H, J = 17.5 Hz), 3.91 (m, 2H), 3.62 (d, 1H, J = 12.1 Hz), 3.55 (d, 1H, J = 12.8 Hz), 3.42 (d, 2H, J = 16.2 Hz), 2.95 (s, 3H), 2.94 (s, 3H), 2.92 (s, 3H), 2.91 (s, 3H), 2.93–2.83 (m, 2H), 2.16–2.10 (m, 2H), 1.70–1.40 (m, 12H), 1.43 (s, 9H), 1.05–0.94 (m, 2H), 0.98 (d, 3H, J = 6.5 Hz), 0.97 (d, 3H, J = 6.5 Hz), 0.85 (d, 3H, J = 6.5 Hz), 0.84 (d, 3H, J = 6.5 Hz), 0.03 (s, 9H); $^{13}\text{C NMR}$ (CDCl_3 , 100 MHz) δ 172.7, 172.1, 169.4, 169.3, 169.2, 169.1, 167.7, 167.6, 167.3, 166.6, 155.0, 79.8, 65.2, 63.9, 62.3, 53.7, 52.9, 52.5, 51.2, 49.5, 49.2, 44.0, 43.8, 41.9, 41.8, 35.0, 34.9, 30.4, 30.3, 29.7, 29.6, 28.5, 28.4, 28.3, 26.8, 26.6, 24.7, 24.6, 20.0, 19.9, 19.4, 19.3, 19.1, 19.0, 10.2, –1.99; IR (KBr) ν_{max} 3324, 2939, 1743, 1672, 1641, 1487, 1456, 1416, 1287, 1251, 1169, 1135, 1016, 849, 732 cm^{-1} ; FABHRMS (NBA–CsI) m/z 1275.4716 ($\text{M} + \text{Cs}^+$, $\text{C}_{50}\text{H}_{86}\text{N}_{10}\text{O}_{16}\text{Si}$ requires 1275.4768).

N^1 -SES- N^6 -[[3-(benzyloxy)quinoly]-2-carbonyl]-D-Ser-Pip-Gly-Sar-NMe-Val)₂ (Serine Hydroxyl) Dilactone (31). A solution of **29** (17.5 mg, 0.015 mmol) in 3 M HCl–EtOAc (1 mL) at 25 °C was stirred for 30 min. The solvent was removed in vacuo to afford the hydrochloride salt **30** (16.5 mg, 16.5 mg theoretical, 100%) as a white powder which was used directly in the next reaction.

A solution of the hydrochloride salt **30** (16.5 mg, 0.015 mmol) and **28**²⁸ (17.1 mg, 0.06 mmol, 4 equiv) in DMF (1 mL) was treated sequentially with NaHCO_3 (14.0 mg, 0.16 mmol, 11 equiv), HOBt (13.1 mg, 0.97 mmol, 6.5 equiv), and EDCI (11.7 mg, 0.06 mmol, 4 equiv), and the reaction mixture was stirred at 25 °C for 48 h. The mixture was diluted with EtOAc (20 mL) and washed with H_2O (10 mL) and saturated aqueous NaCl (10 mL), dried (Na_2SO_4), filtered, and concentrated in vacuo. Flash chromatography (SiO_2 , 1 \times 15 cm, 5% EtOH– CH_2Cl_2) afforded **31** (12.6 mg, 20 mg theoretical, 63%) as a white powder: R_f 0.51 (20% CH_3CN –EtOAc); $[\alpha]_D^{25}$ –84 (c 0.3, CHCl_3); $^1\text{H NMR}$ (CDCl_3 , 400 MHz) δ 9.00 (d, 1H, J = 6.3 Hz), 8.45 (d, 1H, J = 5.7 Hz), 8.43 (d, 1H, J = 5.7 Hz), 7.93 (d, 1H, J = 7.5 Hz), 7.69 (d, 1H, J = 7.6 Hz), 7.60 (s, 1H), 7.58–7.52 (m, 4H), 7.39 (m, 2H), 7.30 (m, 1H), 5.81 (d, 1H, J = 7.0 Hz), 5.45 (d, 1H, J = 16.6 Hz), 5.44 (d, 1H, J = 5.8 Hz), 5.37–5.26 (m, 6H), 4.86 (dd, 1H, J = 2.0, 12.0 Hz), 4.82 (d, 1H, J = 11.0 Hz), 4.79 (d, 1H, J = 11.0 Hz), 4.67–4.61 (m, 2H), 4.59 (dd, 1H, J = 2.7, 12.0 Hz), 4.46–4.35 (m, 3H), 4.04–3.98 (m, 3H), 3.93–3.87 (m, 1H), 3.76 (d, 1H, J = 13.3 Hz), 3.56 (d, 1H, J = 14.3 Hz), 3.48 (d, 1H, J = 16.6 Hz), 3.42 (d, 1H, J = 16.6 Hz), 3.08 (s, 3H), 2.94 (s, 3H), 2.93 (s, 3H), 2.92 (s, 3H), 2.95–2.83 (m, 2H), 2.15–2.04 (m, 2H), 1.75–1.35 (m, 12H), 0.97 (d, 3H, J = 6.6 Hz), 0.95 (d, 3H, J = 6.6 Hz), 0.84 (d, 3H, J = 6.6 Hz), 0.81 (d, 3H, J = 6.6 Hz), 0.04 (s, 9H); $^{13}\text{C NMR}$ (CDCl_3 , 100 MHz) δ 172.7, 172.1, 169.4, 169.2, 169.1, 167.8, 167.7, 167.0, 166.6, 163.5, 151.7, 142.6, 141.6, 136.0, 130.2, 129.5, 128.7, 128.4, 128.0, 127.5, 126.9, 126.4, 117.2, 70.9, 65.2, 62.8, 62.3, 62.2, 53.7, 53.0, 52.4, 50.7, 49.5, 49.3, 49.2, 44.0, 43.8, 41.9, 41.8, 35.0, 34.9, 30.4, 30.3, 29.7, 28.7, 28.4, 26.8, 26.5, 24.8, 24.6, 20.1, 20.0, 19.4, 19.3, 19.1, 19.0, 10.2, –2.0; IR (KBr) ν_{max} 3322, 2936, 1742, 1668, 1639, 1491, 1462, 1285, 1255, 1135, 1015, 874, 734 cm^{-1} ; FABHRMS (NBA–CsI) m/z 1436.6084 ($\text{M} + \text{Cs}^+$, $\text{C}_{62}\text{H}_{89}\text{N}_{11}\text{O}_{16}\text{Si}$ requires 1436.5033).

N^1 -SES- N^6 -[[3-(hydroxyl)quinoly]-2-carbonyl]-D-Ser-Pip-Gly-Sar-NMe-Val)₂ (Serine Hydroxyl) Dilactone (32). A solution of **31** (10 mg, 0.0077 mmol) in 5 mL of EtOAc was treated with 10% Pd–C (4 mg), and the resulting black suspension was stirred at 25 °C under an atmosphere of H_2 (1 atm) for 14 h. The catalyst was removed by filtration through Celite, and the filtrate was concentrated in vacuo. Flash chromatography (SiO_2 , 1 \times 10 cm, 10% CH_3CN –EtOAc) afforded **32** (8.0 mg, 9.3 mg theoretical, 86%) as a white powder: R_f 0.7 (20% CH_3CN –EtOAc); $[\alpha]_D^{25}$ –105 (c 0.3, CHCl_3); $^1\text{H NMR}$ (CDCl_3 , 400 MHz) δ 11.74 (s, 1H, OH), 9.55 (d, 1H, J = 6.4 Hz, Ser⁶–NH), 8.50 (d, 1H, J = 5.0 Hz, Gly⁸–NH), 8.44 (d, 1H, J = 5.0 Hz, Gly³–NH), 7.81 (m, 1H, C5'–H), 7.70 (m, 1H, C8'–H), 7.63 (s, 1H, C4'–H), 7.50 (m, 2H, C6' and C7'–H), 5.81 (d, 1H, J = 7.0 Hz, Ser¹–

NH), 5.55 (d, 1H, Sar⁹- α -CH), 5.54 (d, 1H, $J = 5.1$ Hz, Pip⁷- α -CH), 5.30 (d, 1H, $J = 16.6$ Hz, Sar⁴- α -CH), 5.28 (d, 1H, $J = 4.6$ Hz, Pip²- α -CH), 5.25 (d, 1H, $J = 6.4$ Hz, Ser⁶- α -CH), 4.98 (d, 1H, $J = 11.0$ Hz, Ser⁶- β -CH), 4.86 (d, 1H, $J = 11.0$ Hz, Val¹⁰- α -CH), 4.79 (d, 1H, $J = 11.0$ Hz, Val⁵- α -CH), 4.64 (m, 2H, Ser¹- α and β -CH), 4.45–4.35 (m, 4H, Ser¹- β -CH, Gly³- α -CH, Ser⁶- β -CH, and Gly⁸- α -CH), 4.10–3.99 (m, 3H, Gly³- α -CH, Gly⁸- α -CH, and Pip⁷- ϵ -CH), 3.90 (m, 1H, Pip²- ϵ -CH), 3.72 (d, 1H, $J = 13.0$ Hz, Pip⁷- ϵ -CH), 3.56 (d, 1H, $J = 13.0$ Hz, Pip²- ϵ -CH), 3.55 (d, 1H, $J = 16.6$ Hz, Sar⁹- α -CH), 3.43 (d, 1H, $J = 16.6$ Hz, Sar⁴- α -CH), 3.11 (s, 3H, Val¹⁰-NCH₃), 2.95 (s, 3H, Val⁵-NCH₃), 2.94 (s, 3H, Sar⁹-NCH₃), 2.92 (s, 3H, Sar⁴-NCH₃), 2.89 (m, 2H, SO₂CH₂), 2.12 (d split septet, 1H, $J = 11.0$, 6.5 Hz, Val¹⁰- β -CH), 1.85–1.45 (m, 12H, Pip²- and Pip⁷-(CH₂)₃), 1.01 (m, 2H, CH₂TMS), 0.97 (d, 3H, $J = 6.5$ Hz, Val²- γ -CH₃), 0.92 (d, 3H, $J = 6.5$ Hz, Val¹⁰- γ -CH₃), 0.85 (d, 3H, $J = 6.5$ Hz, Val²- γ -CH₃), 0.79 (d, 3H, $J = 6.5$ Hz, Val¹⁰- γ -CH₃), 0.05 (s, 9H, Si(CH₃)₃); ¹³C NMR (CDCl₃, 100 MHz) δ 172.6, 172.2, 169.4, 169.3, 169.2, 169.1, 167.8, 167.7, 167.6, 166.5, 166.2, 153.8, 141.5, 134.6, 132.1, 129.4, 128.5, 127.1, 126.4, 120.3, 65.2, 62.3, 62.2, 61.9, 53.7, 53.0, 52.4, 50.6, 49.5, 49.3, 49.2, 44.0, 43.9, 41.9, 41.8, 35.0, 34.9, 30.3, 30.2, 28.7, 28.5, 26.8, 26.2, 24.9, 24.6, 20.1, 20.0, 19.5, 19.3, 19.1, 18.7, 10.2, -2.0; IR (KBr) ν_{\max} 3329, 2936, 1744, 1639, 1518, 1462, 1413, 1287, 1255, 1135, 1015, 843, 754 cm⁻¹; UV (CH₃OH) λ_{\max} 202 (43 000), 229 (30 000), 300 (4000), 356 nm (3400); FABHRMS (NBA) m/z 1214.5671 (M + H⁺, C₅₅H₈₃N₁₁O₁₆-SiS requires 1214.5588).

NMR Measurements. All samples were degassed by six freeze–pump–thaw cycles, and all spectra were recorded at 296 K. All 2D spectra were recorded with quadrature detection in both dimensions, TPPI⁴⁶ was used in F₁. The 2D spectra were processed and analyzed with the Felix program (version 2.3.0, BIOSYM Technologies) on a Silicon Graphics Personal IRIS Workstation. The parameters of the individual NMR experiments are given in the following experimentals.

1. 1D ¹H Spectrum: Pulse length, $P_1 = 5.0$ μ s; relaxation delay, $d_1 = 1.0$ s; 128 acquisitions.

2. 1D ¹H–¹H Decoupling Spectrum (Homodecoupler Mode): Pulse length, $P_1 = 10.0$ μ s; relaxation delays, $D_1 = 1$ s, $D_{11} = 1$ ms; the power set for the decoupled nucleus (DEC), dL0 = 50 dB; 64 acquisitions.

3. 2D ¹H–¹H NOESY Spectrum: Sequence $D_1 -90^\circ -t_1 -90^\circ -\tau_{\text{mix}} -90^\circ -t_2$; pulse length (90°), $P_1 = 18$ μ s; delays, $d_0 = 3$ μ s, $d_1 = 2$ s, $d_8 = 450$ ms; sweep width in F₁ and F₂, SWH = 4424.779 Hz; 32 acquisitions; 512 increments.

4. 2D ¹H–¹H ROESY Spectrum: Sequence $D_1 -90^\circ -t_1 -90^\circ -\tau_{\text{mix}} -90^\circ -t_2$; pulse lengths, P_1 (90° transmitter high power pulse) = 18 μ s; P_{15} (CW pulse for ROESY spinlock) = 400 ms; delays, d_0 (incremented delay) = 3 μ s, d_1 (relaxation delay) = 2 s, d_{12} (delay for power switching) = 20 μ s, d_{13} (short delay) = 3 μ s; powers, h11 (ecoupler high power) = 3 dB, h14 (ecoupler low power) = 17 dB; sweep width in F₁ and F₂, SWH = 4424.79 Hz; 32 acquisitions; 512 increments.

DNA Binding Constant Measurements. All fluorescence measurements were conducted on a JASCO FP-777 spectrofluorometer equipped with a Fisons Haake D8 circulated water cooling system. The temperature was maintained at 24 °C throughout the experimental work. A 4 mL quartz cuvette equipped with a Teflon-coated magnetic stir bar was used in all experiments. Calf thymus DNA (Sigma) was dissolved in 10 mM Tris-HCl (pH 7.4) buffer solution containing 75 mM NaCl. The DNA concentration (320 μ M in base pair) was determined by UV ($\epsilon_{260} = 12\,824$ M⁻¹ in base pair). The excitation and emission spectra were recorded with a sample (2 mL) containing 10 mM Tris-HCl (pH 7.4), 75 mM NaCl buffer, and 20 μ L of a DMSO stock solution of agent with a 10 nm slit width in excitation and emission. The final concentration for sandramycin, luzopeptin A, or **32** was 10 μ M. For sandramycin (**1**), the fluorescence emission spectra exhibited a maximum at 530 nm, and the excitation spectrum showed a sharp band at 260 nm and two broad bands at 300 nm and 360 nm, respectively. When excited at 360 nm, only the band at 530 nm was observed in the emission spectrum, and this excitation wavelength was chosen so that the absorbance of DNA would not interfere with that of agent. For the determination of the DNA binding constant of

sandramycin (**1**), a 2 mL of sample containing 10 μ M sandramycin (**1**) was titrated with 20 μ L of calf thymus DNA (320 μ M) solution. The quenching of fluorescence was measured 5 min after each addition of DNA to allow binding equilibration with 360 nm excitation and 530 nm fluorescence. The results graphically represented in Figure 2 were analyzed by Scatchard analysis,³⁸ and the results are summarized in Table 4.

Similar titrations of solutions of luzopeptin A (10 μ M) and **32** (10 μ M) with calf thymus DNA (320 μ M) were conducted with 340 nm excitation/520 nm fluorescence and 400 nm excitation/510 nm fluorescence, respectively, and the results are summarized in Table 4.

DNA Binding Constant Determination for 25. Method A. Calf thymus DNA (1.0×10^{-5} M in base pair) was mixed with ethidium bromide (5.0×10^{-6} M) resulting in a 2:1 ratio of base pair/ethidium in a 10 mM Tris-HCl (pH 7.4), 75 mM NaCl buffer solution (2 mL). The fluorescence was calibrated at 24 °C to 100% F and 0% F with a DNA–ethidium buffer solution and ethidium buffer solution, respectively. The premixed DNA–ethidium solution was titrated with small aliquots of **25** (20–40 μ L of 3 mM **25** in DMSO) and incubated at 24 °C for 30 min prior to each fluorescence measurement. The fluorescence was measured with 545 nm excitation and 595 nm emission with a slit width of 10 nm. The absolute binding constant from three such titrations were determined at 50% ethidium bromide displacement as measured by a drop in fluorescence to 50%. The binding constant of ethidium bromide employed to calculate the absolute binding constant with a competitive or noncompetitive binding model³⁹ was 4.5×10^5 M⁻¹, and the results are summarized in Table 4.

Method B. A 2 mL of sample containing 400 μ L of calf thymus DNA (320 μ M in base pair) with or without the presence of 40 μ L of **25** (3.2×10^{-3} M in DMSO) in 10 mM Tris-HCl (pH 7.4), 75 mM NaCl buffer solution was titrated with small aliquots of sandramycin (1 μ L, 1.0×10^{-3} M in DMSO). The quenching of fluorescence was measured 5 min after each addition of sandramycin with 360 nm excitation and 530 nm fluorescence. The results were analyzed by Scatchard analysis and summarized in Table 4.

General Procedure for Agarose Gel Electrophoresis. Due to the low solubility of the agents in water, all agents were dissolved in DMSO as stock solutions, stored at -20 °C in the dark, and were diluted to the working concentrations in DMSO prior to addition to the DNA solution. A buffered DNA solution containing 0.25 μ g of supercoiled Φ X174 RF I DNA (1.0×10^{-8} M) in 9 μ L of 50 mM Tris-HCl buffer solution (pH 8) was treated with 1 μ L of agent in DMSO (the control DNA was treated with 1 μ L of DMSO). The [agent] to [DNA] base pair ratios were 0.022 (lane 1), 0.033 (2), 0.044 (3), 0.11 (4), 0.22 (5) for luzopeptin A; 0 (6 control DNA), 0.011 (7), 0.022 (8), 0.033 (9), 0.044 (10), 0.066 (11), 0.11 (12) for sandramycin in gel 5A; 0.011 (1), 0.033 (2), 0.066 (3), 0.11 (4) for sandramycin; and 0 (5, control DNA), 0.022 (6), 0.11 (7), 0.22 (8), 0.44 (9), 0.88 (10), 1.74 (11), 2.2 (12) for compound **32** in gel 5B. The reactions were incubated at 25 °C for 1 h and 5 h for gel A and B, respectively, and quenched with 5 μ L of loading buffer formed by mixing Keller buffer (0.4 M Tris-HCl, 0.05 M NaOAc, 0.0125 M EDTA, pH 7.9) with glycerol (40%), sodium dodecyl sulfate (0.4%), and bromophenol blue (0.3%). Electrophoresis was conducted on a 0.9% agarose gel at 90V for 3 h. The gel was stained with 0.1 μ g/mL ethidium bromide, visualized on a UV transilluminator, and photographed using Polaroid T667 black and white instant film and directly recorded on a Millipore Biolmage 60S RFLP system.

DNase I Footprinting. The DNase I footprinting system was obtained from BRL (Life Technologies, Inc.). The ³²P 5'-end-labeled w794 DNA was prepared as previously described.⁴³ Stock solutions of sandramycin were prepared in DMSO. The solutions were stored in the dark at -20 °C and were diluted to working conditions with buffer (10 mM Tris-HCl, pH 7.0; 10 mM KCl; 10 mM MgCl₂; 5 mM CaCl₂) immediately prior to use. The final concentration of DMSO did not exceed 2%.^{6b} A buffered DNA solution (7 μ L) containing the ³²P 5'-end-labeled w794 DNA (5000 cpm) in 10 mM Tris-HCl (pH 7.0), 10 mM KCl, 10 mM MgCl₂, and 5 mM CaCl₂ was treated with 2 μ L of a freshly prepared sandramycin solution and H₂O (1 μ L). The final concentrations of sandramycin were 2 μ M, 10 μ M, and 20 μ M as indicated. The DNA reaction solutions were incubated at 25 °C for 30 min. The DNA cleavage reactions were initiated by the addition of 1 μ L of a stock solution of DNase I (0.1 μ g/mL) containing 1 mM

(46) Marion, D.; Wuthrich, K. *Biochem. Biophys. Res. Commun.* **1983**, *113*, 967.

of dithiothreitol and allowed to proceed for 1 min at 25 °C. The reactions were stopped by addition of 3 M NH₄OAc containing 250 mM EDTA followed by EtOH precipitation and isolation of the DNA. The DNA was resuspended in 8 μL of TE buffer, and formamide dye (6 μL) was added to the supernatant. Prior to electrophoresis, the samples were warmed at 100 °C for 5 min, placed in an ice bath, and centrifuged and the supernatant was loaded onto the gel. Sanger dideoxynucleotide sequencing reactions were run as standards adjacent to the treated DNA. Gel electrophoresis was conducted using a denaturing 8% sequencing gel (19:1 acrylamide-*N,N*-methylenebisacrylamide, 8 M urea). Formamide dye contained xylene cyanol FF (0.03%), bromophenol blue (0.3%), and aqueous Na₂EDTA (8.7%, 250 mM). Electrophoresis running buffer (TBE) contained Tris base (100 mM), boric acid (100 mM), and Na₂EDTA-H₂O (0.2 mM). The gel was prerun for 30 min with formamide dye prior to loading the samples. Autoradiography of the dried gel was carried out at -78 °C using Kodak X-Omat AR film and a Picker Spectra intensifying screen.

Acknowledgment. We gratefully acknowledge the financial support of the National Institutes of Health (CA 41101). We wish to thank H. Cai and D. S. Johnson for Figure 5 and Dr. J. A. Matson (Bristol-Myers Squibb) for a sample of authentic

sandramycin, for copies of its ¹H and ¹³C NMR, and for information regarding its absolute stereochemistry in advance of publication (ref 2).

Supporting Information Available: The 1D ¹H NMR decoupling results that establish the ¹H NMR assignments for **14**, **24**, **25**, and **29**; a table of ¹H NMR assignments for **25** in CDCl₃, THF-*d*₈, CD₃OD, DMF-*d*₇, and DMSO-*d*₆; a figure comparison of the ¹H NMR spectra of **25** and sandramycin (Figure 6); a figure of the excitation and emission spectra of **1**, luzopeptin A, and **32** (Figure 7); tables of the nucleic acid and sandramycin proton chemical shift assignments in the d(G-CATGC)₂-sandramycin complex and their comparisons with free agent, free DNA, and the analogous luzopeptin A complexes^{29,30} as well as the X-ray crystal structure data for **25** (21 pages). This material is contained in many libraries on microfiche, immediately follows this article in the microfilm version of the journal, can be ordered from the ACS, and can be downloaded from the Internet; see any current masthead page for ordering information and Internet access instructions.

JA952799Y